The Global Atmosphere Watch Precision Filter Radiometer (GAW-PFR) Network for Aerosol Optical Depth long term measurements

Final report

Stelios Kazadzis, Senior Researcher

N. Kouremeti, J. Gröbner

Physikalisch-Meteorologisches Observatorium Davos, World Radiation Center

Funding: Bundesamt für Meteorologie und Klimatologie MeteoSchweiz (11.2018 – 03.2021)

Summary

Aerosol optical depth (AOD) is the single most comprehensive variable to assess the aerosol load of the atmosphere and the most important parameter related to aerosol radiative forcing studies. Multi-wavelength AOD has been defined as an essential climate variable from various global bodies and agencies such as the Global Climate Observing System the Global Atmosphere Watch (GAW) Program of the World Meteorological Organization, the European Space Agency Climate Change Initiative and others.

Ground-based sun-photometers have been deployed during the last 20-25 years in order to provide long term series of AOD measurements at various locations. PMOD/WRC during the 90's has developed the Precision Filter Radiometer (PFR) that has been used for long term AOD measurements under a GAW-PFR Network of sun-photometers started in Davos Switzerland and from 1999 at other locations, worldwide. Currently, more than 40 PFR instruments are operating worldwide. 15 of them are measuring in locations defined as core GAW-PFR sites by the WMO Scientific Advisory Group for aerosols and maintained/calibrated by PMOD/WRC. The remaining instruments owned by research institutes are also associated with PMOD/WRC as they are regularly calibrated by the WRC section WORCC that is the WMO defined World Aerosol Optical depth Research and Calibration Center.

In line with the Strategic Priority 1.2, of the GCOS Switzerland Strategy 2017-2026, the Swiss based GAW-PFR aerosol monitoring network moderated by PMOD-WRC, measuring the GCOS related Essential Climate Variable (spectral aerosol optical depth), has accomplished the following goals within this project:

To homogenize the time GAW-PFR Aerosol Optical depth time series

This task was achieved by partly re-evaluating the calibration procedures and apply them to the past aerosol data. Also, new and improved post correction algorithms have been developed and used. For example, an improvement on the cloud detection algorithm (Kazadzis et al., 2018a). This procedure included the recalculation of the aerosol optical depth time series on a minute level. Visual inspection of past data helped assessing the inclusion of episodic aerosol events in the aerosol database. There were no major changes in the absolute level of the calculated AOD, however a number of data have been discarded after applying the new procedures.

To provide to an uncertainty estimation of AOD GAW-PFR network measurements and to contribute to the GCOS review of essential climate variables (ECV) for multi-wavelength AOD.

A main aspect was to calculate an uncertainty estimation for the AOD time series, based on the data re-evaluation. This is an important aspect that is a mandatory requirement for GCOS and WMO-GAW related aerosol products. This uncertainty estimation was compared with WMO related uncertainties (±0.005 + 0.01/m optical depths), where m is the air mass and the GCOS related AOD/ECV uncertainty that is defined as a maximum of 0.03 in AOD or 10% and equal or less than 0.02 per decade for trend analysis studies. Main assessment of the uncertainty included uncertainty sources related with: PFR measurements, the calibration procedures and hierarchy, absorbing gases (Ozone, NO_2), the correction for Rayleigh scattering and the effects of aerosol forward scattering to the AOD retrieval due to the instrument field of view.

GCOS is currently reviewing and will update the requirements as part of their contribution to the UNFCCC Global stock take. In this direction, results and experience gained from this GAW-PFR project were used for the definition of the

new requirements that are under review. This project's PI is the main author of the, under discussion with the relative users, GCOS requirements for AOD.

To provide an assessment of the long term stability of the GAW-PFR measurements and the accuracy of the aerosol optical depth series.

A comprehensive comparison of more than 70K synchronous 1 min aerosol optical depth (AOD) measurements from three GAW-PFRs traceable to the World AOD reference, and 15 Aerosol Robotic Network Cimel radiometers (AERONET-Cimel), calibrated individually, was performed in the period 2005–2015. The goal of this study is to assess whether, despite the marked technical differences between both networks (AERONET, GAW-PFR) and the number of instruments used, their long-term AOD data are comparable and consistent. The percentage of data meeting the WMO traceability requirements (95 % of the AOD differences of an instrument compared to the WMO standards lie within specific limits) is >92 % at 380 nm, >95 % at 440 nm and 500 nm, and 98 % at 870 nm. For the data outside these limits, the contribution of calibration and differences in the calculation of the optical depth contribution due to Rayleigh scattering and O_3 and NO_2 absorption have a negligible impact. For AOD >0.1, a small but non-negligible percentage (~1.9 %) of the AOD data outside the WMO limits at 380 nm can be partly assigned to the impact of dust aerosol forward scattering on the AOD calculation due to the different field of view of the instruments. The comparison of the Ångström exponent (AE) shows that under non-pristine conditions (AOD >0.03 and AE <1) the AE differences remain very low (<0.1). This long-term comparison shows an excellent traceability of AERONET-Cimel AOD with the World AOD reference at 440, 500 and 870 nm channels and a fairly good agreement at 380 nm. (Relative publication: Cuevas et al., 2019). Results of previous international intercomparison campaigns among PFRs and reference sun-photometers of other networks have been also used (2015 Filter Radiometer Comparison – Kazadzis et al., 2018b and the SKYNET network – Nakajima et al., 2020).

Re-evaluation of the GCOS-PFR network instrumentation strategy.

Three stations with technical and local/national organization problems have been substituted by PFR Associated stations with long term series, based on data quality criteria. The Valentia, Ireland station and the Troll, Antarctic station (started both in 2007) and the Marambio, Antarctic station (2005) has been added to the core GAW-PFR stations. In addition, links of GAW and GAW-PFR with global networks such as AERONET and SKYNET and research infrastructures (ACTRIS) have been established. PFR instruments will be installed during 2020-21 in three of the main ACTRIS-AERONET and SKYNET sites. Major role in the GAW-PFR instrument strategy re-evaluation was the decision of PMOD-WRC to build new series of PFR instruments, with improved electronics and input optics. Results of this project have been crucial for this decision. The new instrument series started to be constructed in mid-2019 and will be ready in the end of 2020. They will gradually substitute the existing core GAW-PFR instruments until the end of 2022.

GAW-PFR AOD climatology

During this phase we have calculated statistics for AOD at 4 wavelengths and Ångström Exponent (AE) for each of the 15 GAW-PFR station long term series. Including, the time series monthly and daily AODs and AE. Their intra-annual variability, the relative frequency distribution of the observed AODs together with the arithmetic mean and standard deviation and the geometrical mean and geometrical standard deviation of the distributions. Finally, the relationship of AOD at 500nm and the AE for daily averaged measurements. An example can be seen in the figure 1 below for Jungfraujoch, Switzerland station.

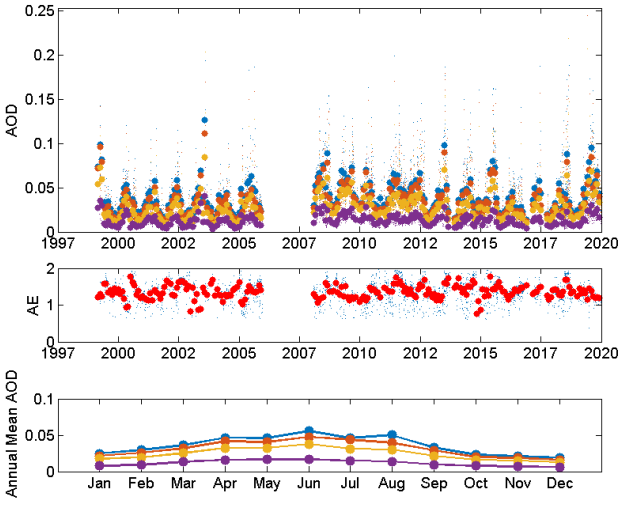

Period (Days) 1999 - 2019 (3020)

JUNGFRAUJOCH, Switzerland

	Mean AOD ± std	Gm	med	Prc. 20 - 80
500nm	0.029 ± 0.020	0.025 /* 1.766	0.024	0.015 - 0.039
862nm	0.014 ± 0.010	0.012 /* 1.849	0.011	0.007 - 0.020
AE	1.350 ± 0.286	1.316 /* 1.263	1.375	1.110 - 1.598

Figure 1: time series of AOD at 4 wavelengths (up), AE (middle), AOD intra-annual (down) and station statistics (right) for Jungfraujoch, Switzerland station.

High mountain stations of Mauna Loa, USA (MLO), Jungfraujoch, Switzerland (JFJ) and Izana, Spain (IZO) showed the lowest AOD (0.018, 0.029, 0.049 for AOD_{500nm} respectively) values with the IZO measurements to show higher AODs and lower AEs at Saharan intrusion periods. M. Walliguan, China (WLG) station exhibited very high AODs and low AEs for a 4Km altitude stations. However, WLG is also affected by dust intrusions from middle China regions. AEs JFJ, MLO and Davos (DAV) were found to be 1.3 to 1.4 that follow the Angstrom's suggestion for natural aerosols. Alice Springs, Australia (ASP) station had also low AOD_{500nm} values (0.056). The annual variation of AOD shows the standard pattern of low/high values in Austral winter/summer. Minimal daily means are comparable to high altitude stations in the northern hemisphere.

Most stations show larger AOD values in the summer than in winter months, with maximal values typically between spring and summer as rapid heating of the ground in spring and early summer leads to greater vertical instability, and consequently dust and combustion products are carried most effectively from ground to the atmosphere.

Aerosol optical depth at polar stations Ny Ålesund (NYA) is usually higher during spring than in summer. Spring time AODs at NYA are 2-3 times larger than the ones in the south polar stations of Marambio (MBI) and Troll (TRO). This is due to the Arctic haze phenomenon when aerosol removal mechanisms are suppressed and the cold and stable winter Arctic boundary layer may extend over anthropogenic sources in the south.

GAW-PFR climatology results have been presented in the American and European Geophysical Union conferences (AGU, December 2019 San Francisco, USA and EGU, May 2020 on-line).

Trend analysis of 15 core GAW- PFR stations

Measurement series of 15-20 years (8 stations), 10-15 years (5 stations) and 2 stations with less than 10 years of data, have been analyzed. Trend analysis was performed using two independent methods commonly used in the literature:

The monthly/seasonal Kendall test, a generalization of the Mann-Kendall (MK) test, a non-parametric test that can be applied to time-series with seasonal cycles and missing values. The slope (trend) is determined by Sen's method. Data used were daily values of AODs, and AEs from each GAW-PFR station.

The Weatherhead et al., 1998 (WH) statistical method of trend detection that takes into account the magnitude of variability and autocorrelation of the noise in the data. Data used were monthly mean, median and geometrical mean of AODs (three different approaches) at four wavelengths and AEs.

Using the MK test only 4 stations showed positive trends while none of them statistically significant ones. The remaining 11 stations showed generally small but negative trends all of them lower than 2% per year or 0.02 in AOD_{500nm} units per decade. High mountain stations showed small but negative trends (IZO, MLO, WLG) while JFJ showed a small but positive. In the cases of MLO, IZO and JFJ the AOD trend per decade is 0.001. 4 and 5 stations showed statistically significant trends for 500nm and 865nm wavelengths respectively. Low trend values should be treated with caution as long as they fall well within the PFR uncertainty limits.

The WH results for mean, median and geometrical mean have been compared with the MK results. 13 out of 15 stations show an agreement on the trend sign for both methods (all three for WH and the MK). The two disagreeing stations did not have statistical significant trends for all methods. The agreement of the independent methods used gives more confidence on the result interpretation. MK result summary is presented in the following map.

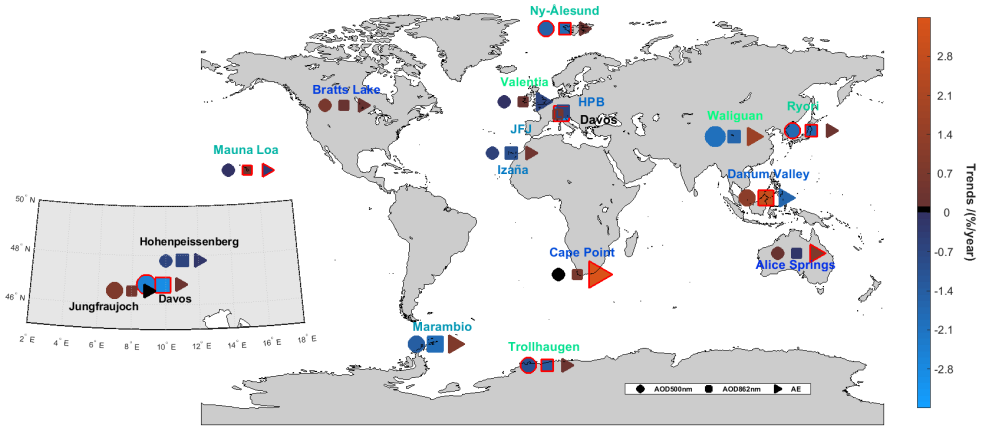

Map of trends per year for AOD at 500 (circle) and 865nm (box) and AE (triangle) using the MK test. Red outlined points show the 95% statistical significant values

Data submission in an open access database (WDCA)

GAW-PFR data are submitted regularly to world data center for aerosols WDCA. Real time data are sent in a daily basis. The current real time data utilize the new calibrations and QA/QC procedures that have been defined within this project. Data submission of recalibrated data to WDCA is performed according to WMO rules: full yearly dataset is submitted until the end of the following year unless a recalibration is pending (in this case immediately after the recalibration analysis).

Additional PFR stations mentioned here (Valentia/Ireland, Marambio and Troll/Antarctica) have been also started submitting data to the WDCA. One-minute data are not yet available in WDCA as at the moment hourly data are the maximum frequency data. New data series for all data from the GAW-PFR network are anticipated to be submitted and appear in the World Data Center for Aerosols till the end of 2020.

Outreach

- Presentation at the American Geophysical Union fall meeting, December, 2019 – San Francisco, USA. Aerosol Kazadzis S. et al., Optical Depth Measurements at the WMO Global Atmospheric Watch - PFR Network Stations
- Kazadzis, S., Kouremeti, N., and Gröbner, J.: Aerosol Optical Depth Measurements at high altitude and polar WMO Global Atmospheric Watch - PFR Network Stations, EGU General Assembly 2020, Online, 4–8 May 2020, EGU2020-6161, https://doi.org/10.5194/egusphere-egu2020-6161, 2020

Online presentation: https://meetingorganizer.copernicus.org/EGU2020/EGU2020-6161.html

- The GAW-PFR network climatology and trends – PMODWRC Science meeting 07.2020, S. Kazadzis

Publications

- Cuevas, E., Romero-Campos, P. M., Kouremeti, N., Kazadzis, S., Räisänen, P., García, R. D., Barreto, A., Guirado-Fuentes, C., Ramos, R., Toledano, C., Almansa, F., and Gröbner, J.: Aerosol optical depth comparison between GAW-PFR and AERONET-Cimel radiometers from long-term (2005–2015) 1 min synchronous measurements, Atmos. Meas. Tech., 12, 4309–4337, https://doi.org/10.5194/amt-12-4309-2019, 2019.
- Nakajima, T., Campanelli, M., Che, H., Estellés, V., Irie, H., Kim, S.-W., Kim, J., Liu, D., Nishizawa, T., Pandithurai, G., Soni, V. K., Thana, B., Tugjsurn, N.-U., Aoki, K., Hashimoto, M., Higurashi, A., Kazadzis, S., Khatri, P., Kouremeti, N., Kudo, R., Marenco, F., Momoi, M., Ningombam, S. S., Ryder, C. L., and Uchiyama, A.: An overview and issues of the sky radiometer technology and SKYNET, Atmos. Meas. Tech. Discuss., https://doi.org/10.5194/amt-2020-72, 2020
- Kazadzis S. and co-authors, Aerosol climatology and trends from the GAW-PFR aerosol network. To be submitted in September, 2020

Acknowledgment: S. Kazadzis would like to thank: All GAW-PFR stations local operators for their commitment in keeping the network in good quality for the past 20 years. Dr. Martine Collaud Coen for the provision MK test and Sen's slope software and her help on result interpretation. Dr. C. Wehrli for his work on the PFR instrument design and operation and the GAW-PFR network initiation.

Project scientific report

Introduction

Growing recognition of the role of atmospheric aerosols in the determination and modification of the Earth's radiation budget and hydrological cycle through their direct and indirect effects has led to a steady increase of scientific interest in aerosol physical, chemical and optical properties over the last decades (e.g. Augustine et al., 2008). Aerosols are an important climate forcing agent with the magnitude of aerosol forcing to be –0.45 (–0.95 to +0.05) Wm^{-2} for aerosol alone and –0.9 (–1.9 to –0.1) Wm^{-2} when aerosol/cloud feedbacks were accounted for, as reported in the past IPCC report (IPCC, 2013). Based on the same report, the impact of aerosols on the Earth-atmosphere radiation budget is still considered as one of the most significant and uncertain aspects. Aerosol optical depth (AOD) is the most comprehensive variable to assess the aerosol load of the atmosphere (WMO, 2003, 2005) and the most important parameter related to aerosol radiative forcing studies. The second aerosol optical parameter in importance is the Ångström exponent (AE) that accounts for the spectral dependency of the AOD. AOD is one of the core aerosol parameters of the World Meteorological Organization (WMO, 2003), Global Atmosphere Watch (GAW) program. In addition, it is defined as an Essential Climate Variable (ECV) for atmospheric composition from the Global Climate Observing System (GCOS) and as a variable that critically contributes to the characterization of Earth's climate. Furthermore, European Space Agency related ECVs include mainly AOD as one of the major physical, chemical or biological variables that critically contributes to the characterization of Earth's climate.

AOD and AE can be derived from the ground with measurements of the spectral transmission of direct solar radiation by sun-photometers. Ground-based sun-photometers have been deployed during the last 20-25 years in order to provide long term series of AOD measurements at various locations (Holben, 2001, Che et al., 2015, Goloub et al., 2007, Mitchell et al., 2017, Nakajima et al., 2020). Several AOD intercomparison campaigns with the participation of reference instruments that belong to the above networks, have taken place as short-term intensive field campaigns or long term campaigns and have proven themselves a successful method of relating the methodologies of standards from one network to another on deriving AOD (e.g. Kazadzis et al., 2018b).

A global network of aerosol optical depth (AOD) observations was started in 1999 by PMOD/WRC in collaboration with GAW Global Observatories as proposed by the WMO Scientific Advisory Group for Aerosols (SAG/Aerosols) and funded by MeteoSwiss. During an initial trial-phase, this network served as a test-bed for new instrumentation and methods of calibration and determination of AOD in GAW, after WMO had recommended to abandon AOD observations in the former BAPMoN program, following a critical review of measurement procedures and data quality assurance in 1994. A World Optical Depth Research and Calibration Center (WORCC) was established in 1996 at PMOD/WRC, based on a mandate of WMO. PMOD/WRC during the 90's has developed the Precision Filter Radiometer (PFR) (Wehrli, 2000) that has been used for long term AOD measurements under a GAW-PFR Network of sun-photometers started at Davos Switzerland and from 1999 at other locations, worldwide. Currently, more than 40 PFR instruments are operating worldwide. 15 of them are located in core locations defined by the WMO Scientific Advisory Group for aerosols and maintained/calibrated by PMOD/WRC. The remaining instruments owned by scientific institutes and meteorological agencies, are also associated with PMOD/WRC, as they are regularly calibrated by the World Radiation Center (WRC) section of the WMO defined World aerosol Optical depth Research and Calibration Center (WORCC).

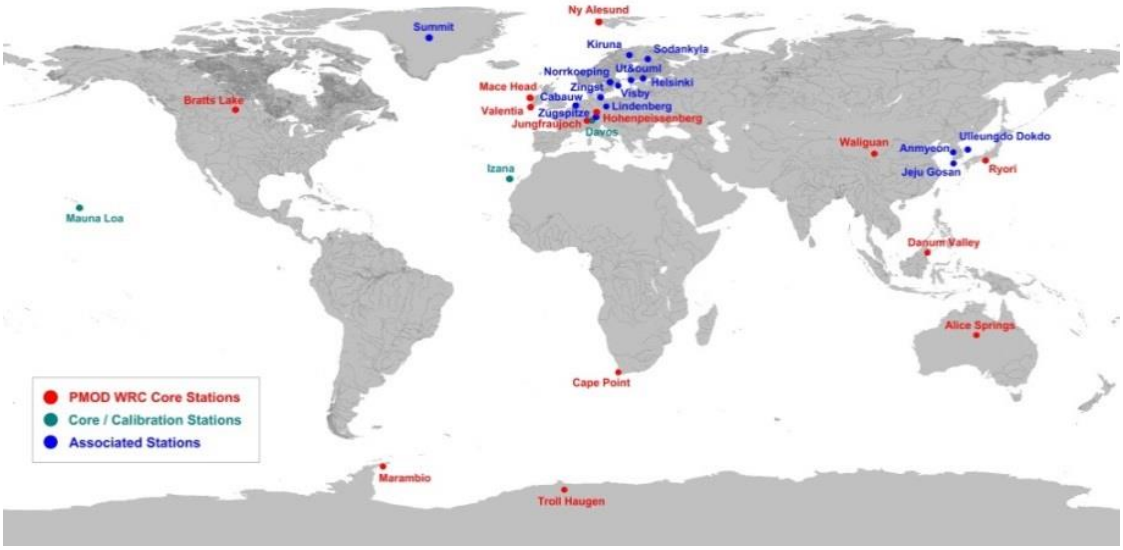

Map of the GAW-PFR monitoring stations

Out of the 15 GAW-PFR stations 8 have 15 or more years and another 5 have 10 or more years of AOD measurements. More details about the calibration procedure and the instrument locations and measurement periods can be found in Kazadzis et al., 2018a. Instrument/location table can be found below.

Table: GAW-PFR station details, location characteristics and AOD time-series information.

Station (abbreviation)	Lat.	Lon.	Alt. (m)	Country	Type of Location	Main Types of Air-Masses	Time-Series	Previous studies
Alice Springs (ASP)	23.80°S	133.87°E	547	Australia	desert	remote continental	2002 – 2019	*Mitchell et al. 2017*
Bratts Lake (BRA)	50.28°N	104.70°W	576	Canada	prairie, agricultural	remote continental	2001 – 2012	*McArthur et al. 2003*
Davos (DAV)	46.55N	7.98E	1590	Switzerland	Alpine rural	rural	2003 – 2019	*Nyeki et al. 2012*
Danum Valley (MAL)	4.98°N	117.84°E	436	Malaysia	tropical forest	remote continental	2007-2017	*Nyeki et al. 2012*
Hohenpeissenberg HPB)	47.80°N	11.02°E	995	Germany	pre-alpine, rural	rural	1999 – 2019	*Ruckstuhl (2008); Nyeki(2012)*
Izana (IZO)	28.31°N	16.50°E	2371	Spain	island	free-troposphere	2001 – 2019	*Barreto et al. 2014*
Jungfraujoch (JFJ)	46.55°N	7.99°N	3580	Switzerland	high-alpine	free-troposphere	1999 – 2019	*Ruckstuhl (2008); Nyeki(2012)*
Mauna Loa (MLO)	19.53°N	155.58°W	3397	USA	island	free-troposphere	2000 – 2019	*Dutton et al. 1994*
Ny Ålesund (NYA)	78.91°N	11.88°N	17	Svalbard	Arctic coast, island	Arctic/marine, BL	2002 – 2019	*Herber et al. 2002*
Ryori (RYO)	39.03°N	141.83°E	230	Japan	coast	marine boundary layer	2002 – 2018	
Cape Point (CPT)	34.35°S	18.49°E	230	S. Africa	coast	marine boundary layer	2007- 2019	*Nyeki et al. 2015*
Mt. Waliguan (WLG)	36.28°N	100.90°E	3810	China	high-mountain	free-troposphere	2007- 2019	*Che et al. 2011*
Valentia (VAL)	51.94°N,	10.24°W	24	Ireland	coast	marine boundary layer	2007 – 2019	
Marambio (MAR)	64.24°S	56.62°W	205	Argentina	coast	marine boundary layer	2005 – 2019	*Tomasi et al. 2015*
Troll (TRO)	72.01°S,	2.54°E	1309	Antartica	polar	free-troposphere	2012-present	*Tomasi et al. 2015*

Project activities and research

Harmonization, re-evaluation of AOD data series

During the first phase of the project a work towards a harmonization of the GAW-PFR Network measurements have been performed. This task included different actions:

1. *The re-calibration and re-evaluation for each particular instrument/station.*

GAW - PFR calibration hierarchy consist of the use of the World Optical depth Research and Calibration Center reference. This reference is based on the average of three (triad) well maintained precision filter radiometers (PFRs) that are located at Davos, Switzerland. In addition, Instruments operating in high mountain stations such as Mauna Loa-USA and Izaña-Canary Islands, Spain are performing Langley calibrations and they are transported (one instrument every six months) to WORCC/Davos in order to check the triad stability with an independent instrument/method. Analysis of these scheduled comparisons showed differences less than 1% for most cases. In addition, the average differences of each triad-PFR compared with the triad average was less than 0.003 (in AOD) in more than 99% of the cases, based on 1 minute measurements since 2005 (fig. 1). This number is well below the WMO related limits uncertainty limits. So no changes have been introduced to the triad data set with the exception of a few sporadic measurements (10 days) when one of the triad instruments presented some small but larger than usual deviations. The instrument was maintained and returned to its normal measurement schedule.

Calibrations of the instruments of the GAW-PFR network have been re-visited. In cases that the difference of each instrument's two consecutive calibrations (comparison with the triad) was more than 1% a linear change of the calibration constant was introduced. In some of the cases where Langley calibrations were possible on site, such measurements were used in order to detect if the change was linear or a step change had to be introduced. Finally, all calibration files of all instruments have been calculated.

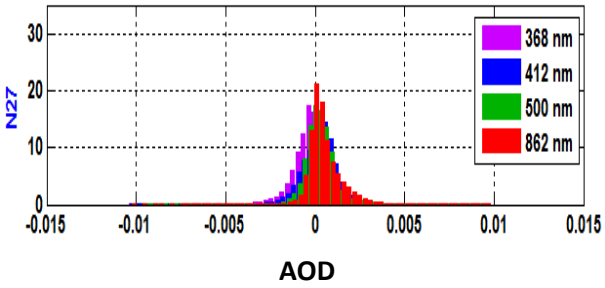

Figure 1: Frequency distribution of the differences of PFR N27 (2005-2016) with the mean of the PFR triad at the four PFR wavelengths.

Recalibration quality assurance and quality control of the stations that were added to the core GAW-PFR group after the results of the spatial gap analysis was also performed. This task included the calibration, QA/QC and cloud flagging procedures for stations (Valentia, Ireland (VTO), Marambio and Troll Antarctica (MBI) and recent measurements of the associated Summit (SUM) station Greenland.

Statistical analysis of minute-daily-monthly data have helped on identifying some inconsistencies in the data series of some of the stations. Cloud rejection procedures were the main reason for such isolated discrepancies. Such data were corrected or discarded.

Comparing instruments that have performed Langley calibrations and also were compared with the triad, can be tricky as small calibration constant changes can be due to the instrument travelling. However, instruments for stations like Alice Springs, (Australia), Ny Alesund (Norway) and Jungfraujoch, (Switzerland) showed calibration differences within 2% for long term periods (Fig. 2).

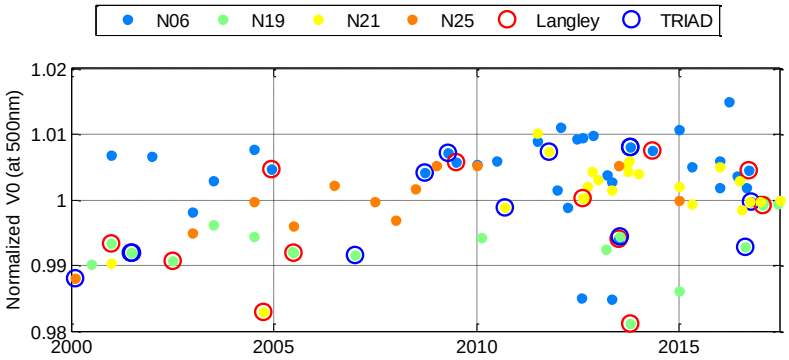

Figure 2: Calibration ratios for 4 different instruments normalized with the last calibration results. Triad and Langley calibrations are shown in circles.

2. *The re-evaluation of AOD, based on changes related to the total column ozone and NO_2 time series.*

Since total column ozone (TOC) absorption affects the AOD retrieval calculations, we used updated (re-evaluated ozone measurements at the sites, if existing, or satellite based TOC retrievals) in order to improve the final AOD product. In addition, we investigated the effect of NO_2 absorption in the AOD retrieval algorithm. GAW-PFR related sites for 412 nm and 368 nm AODs and average columnar NO_2 concentration have been investigated.

Total column ozone values are needed to correct optical depth at 500 nm for ozone absorption. For the rest three wavelength the effect of ozone is negligible. As the absorption coefficient at 500 nm is low, total ozone needs to be known to ±30 Dobson units, or 10% of typical values, for an uncertainty of ±0.001 optical depths at 500 nm. GAW-PFR uses (AURA) satellite overpass observations by the ozone monitoring instrument (OMI) for daily operations (McPeters et al., 2015). For the near real time processing of the AOD data, an ozone climatology is used as OMI overpass data are not available in real time. For the calculation of final AOD data for all GAW – PFR stations OMI overpass ozone is used.

OMI values can be validated using in-situ ozone observations for stations operating a Dobson or Brewer instrument. Where available, total column ozone may be found at the World Ozone and Ultraviolet Radiation Data Centre database (www.woudc.org). Figure 3 shows the evolution of daily mean ozone values at Davos, Switzerland as measured in situ with a Brewer spectrophotometer, and from the OMI ozone retrieval.

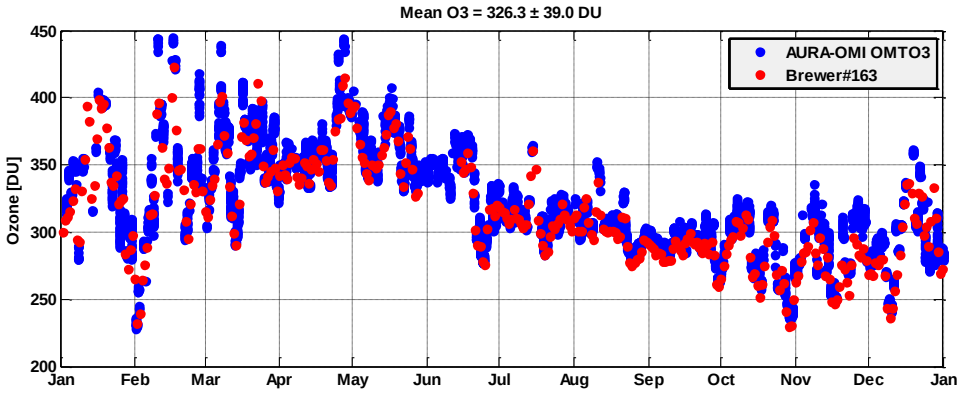

Figure 3. Brewer and OMI ozone values for Davos, Switzerland, 2016

Mean differences are in the order of ±10 D.U. which introduces an uncertainty of ±0.0003 for 500nm. This is very low compared with mean AOD values at Davos which are ~500 times higher. Vaskuri et al., 2018 have also reported on the uncertainties of daily ozone retrieval in the order of ±10DU including the ozone diurnal variations. It has to be noted that the ±39 D.U. standard deviation of the Davos series during 2016 equals to 0.0014 uncertainty in AOD even if the mean (326.3 D.U.) TOC value for Davos is constantly used.

We have calculated the monthly NO_2 concentrations from SCIAMACHY (2002-2012) time series (Boersma et al., 2004). The NO_2 climatology and the NO_2 related contribution to optical depth (OD) for 368nm is shown in figure 4.

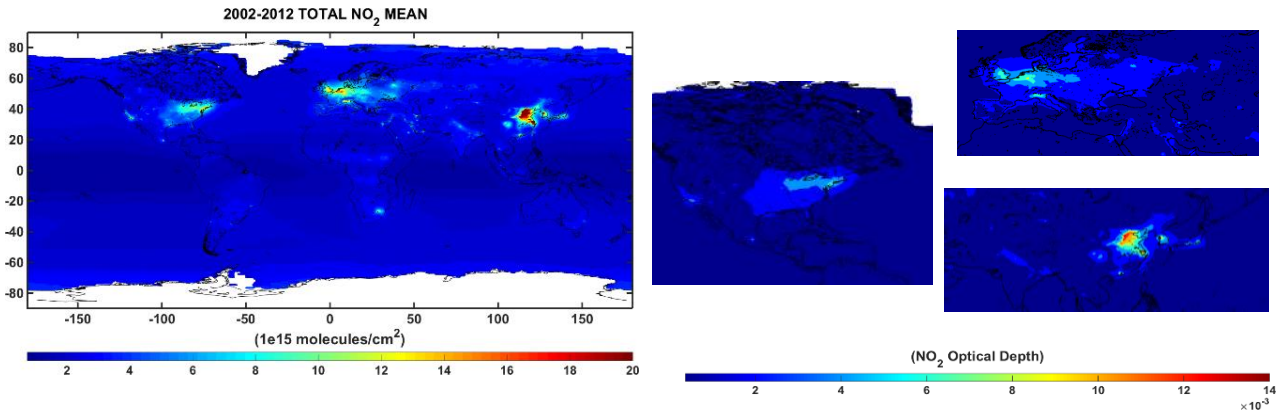

Figure 4: Total NO_2 column from Sciamachy sensor (left) for 2002-2012. Mean NO_2 optical depth for 368 nm (right) for N. America, Europe and Asia.

The Climatology used included monthly mean observations with a resolution of 0.25 X 0.25 degrees. The NO_2 optical depth for 368nm is more than 0.002 only in parts of N. America (0 – 0.006), Europe (0 – 0.008) and Asia (0 – 0.014). So NO_2 have to be considered especially in Eastern Asian region when AOD is calculated.

In addition, an investigation for the GAW-PFR related locations of the contribution of NO_2 absorption to the total OD have been performed. All stations but one have a mean NO_2 in the order of 2 - $4*10^{15}$ mol/cm^2 which is ~0.75-1.5 Dobson Units (Fig. 5). Hohenpeisenberg station, Germany has the highest NO_2 concentration of all GAW-PFR network ones, with mean values of 0.24 ± 0.02 (2σ) D.U. (fig. 5). This is leading to an NO_2 contribution to total AOD of ~0.003 for 368nm and 412nm, ~0.001 for 500nm and ~$1.7*10^{-6}$ for 865nm. It has to be noted that the mean AOD for Hohenpeisenberg station, Germany at 368nm is ~0.15.

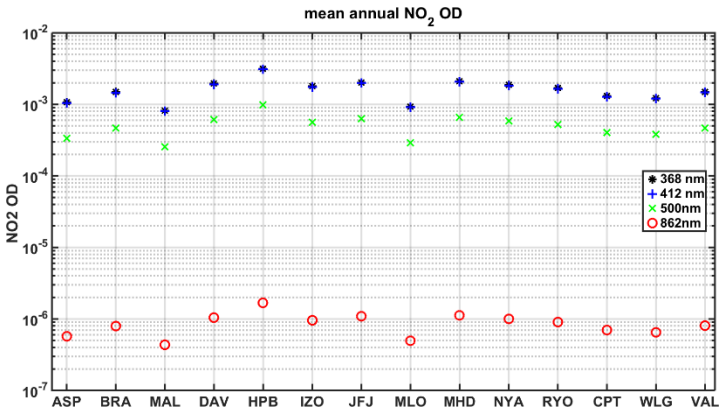

Figure 5. NO_2 mean Optical depth for the GAW-PFR measuring stations.

The NO_2 contribution to the total AOD for the GAW-PFR sites can be considered negligible, however we have decided to include these monthly based calculated corrections.

3. *Cloud filtering update*

The QA/QC algorithms and the additional post processing quality control tests are described in Kazadzis et al., 2018a. The algorithm can provide different cloud flags that correspond to cloudless, thin clouds, thick clouds for every one minute AOD measurement, based on a combination of already established algorithms. Such inclusion could be crucial for AOD future users as recent intercomparison AOD campaigns, including different instrument and cloud algorithms used, showed potential discrepancies on the final AOD datasets (Kazadzis et al., 2018b). In this section we are showing additional cloud flagging algorithms used for the improvement of the AOD data quality.

As AOD measurements cannot be performed under cloudy conditions, a cloud detection algorithm is used for the PFR measurements. Till now three different criteria are used:

- The instrument signal derivative with respect to air mass is always negative. The method has been developed and described in detail by Harrison and Michalsky (1994). For cases when air mass values < 2 and the influence of clouds on the noon-side of perturbations cannot be easily detected, we compare the derivative with the estimate of the clear Rayleigh atmosphere and flag it as cloudy if the rate of change is twice as much (objective method).
- The use of a test for optically 'thick' clouds with AOD_{500nm} >2.
- The use of the Smirnov triplet measurement (Smirnov et al., 2000) by calculating AOD and looking at the signal variability for three consecutive minutes (triplet method).

In order to improve the algorithm and decrease the possibility of including cloud contaminated measurements in the final AOD series we have introduced some additional criteria and tests.

The first test has to do with the variability of the direct sun signal in the 10 minutes (five minutes before and after the individual measurement). There if the variability is more than 0.5% compared with a cloudless sky model then the measurement is considered cloudy. The time window can decrease in cases of obvious cloud contamination in the start or the end of the 10-minute period.

The second test is a check on the direct sun levels compared with a clear sky model. This in order to avoid overcast cloudy but not so variable in terms of direct solar irradiance conditions. Finally, a criterion based on the Ängström exponent (AE) has been included, by checking the AE series variability within a day.

An example of the new cloud flagging algorithm compared to the one before the introduction of the additional checks can be seen in the next figure 6.

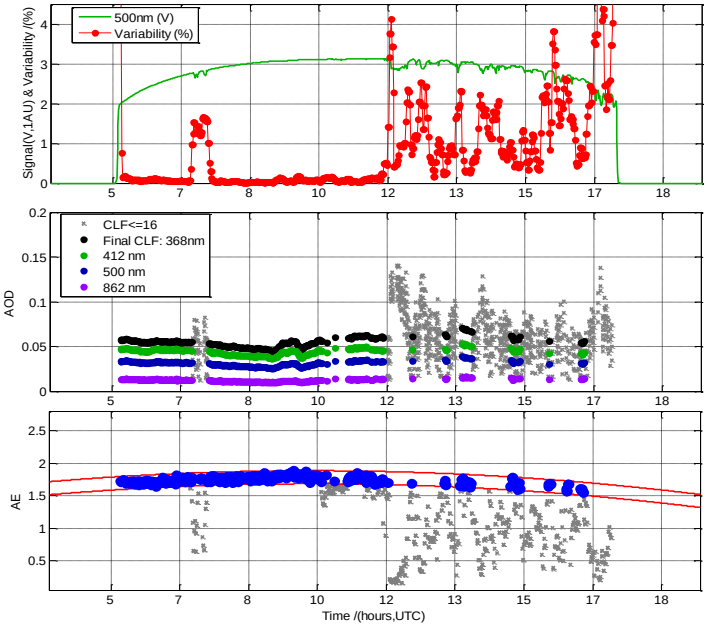

figure 6

Up: PFR signal within one day at 500nm (green) and 10 minute variability (red)

Middle: AOD calculated in 4 wavelengths (colors). Grey AODs have been characterized as cloudless based on the old algorithm and cloudy with the additional criteria.

Lower: Same as middle including the AE criteria.

It has to be noted that depending on if the old or new criteria that are fulfilled or not, each of the cloud flagged minutes is accompanied by a number that provides information on the cloud criteria that have been introduced.

AOD uncertainty estimation

A main aspect of the project was to calculate an uncertainty estimation for the AOD time series, based on the data re-evaluation. This is an important aspect that is a mandatory requirement for GCOS and WMO-GAW related aerosol products. This uncertainty estimation was compared with WMO related uncertainties (±0.005 + 0.01/m optical depths), where m is the air mass and the GCOS related AOD/ECV uncertainty that is defined as a maximum of 0.03 in AOD or 10% and equal or less than 0.02 per decade for trend analysis studies.

Main assessment of the uncertainty included uncertainty sources related with: PFR measurements, the calibration procedures and hierarchy, absorbing gases (Ozone, NO_2), the correction for Rayleigh scattering and the effects of aerosol forward scattering to the AOD retrieval due to the instrument field of view. It has to be noted that in all cases the uncertainty is less that the GCOS recommended uncertainty.

The spectral aerosol optical depth is calculated using the Beer Lambert law:

$$\tau_{aod} = \left[\log\left(\frac{I}{Io}\right) + \left(\tau_{ray} m_{ray} + \sum_i \tau_i m_i\right)\right]/m \qquad (1)$$

τ_{aod}: the aerosol optical depth (AOD) at wavelength λ

For the PFRs: I: PFR signal in Volts, Io: PFR calibration constant in Volts

τ_{ray}: the molecular (Rayleigh) optical depth at wavelength λ using the *Nicolet (1984).*

$$\tau_{ray} = 4.02\text{e}-28./\lambda.\hat{}(4 + 0.389 * \lambda + 0.09426/\lambda - 0.3228) * (2.154\text{e}25).* \text{Pressure}/1013.25;$$

Where λ the wavelength in μm, Pressure = Pressure from PFR internal sensor

m_{ray}: Assuming aerosol layer at 3km , $\sum_i \tau_i m_i = \tau_{O3} * m_{O3} + \tau_{NO2} * m_{NO2}$

τ_{O3}: the ozone optical depth using the ozone cross sections at -45°C

$m, m_{\tau ray}$: the airmass of AOD and Rayleigh scattering at effective height 5km

m_{O3}: the ozone airmass with ozone effective height 22km

The following sources have been considered in the uncertainty analysis including k=1 uncertainty estimation:

Source	**Uncertainty**	**Impact on**	**δAOD (wavelengths(nm))**
1. Measurement & tracking	0.0025	Meas. Voltage/AOD	0.0025/ m
2. calibration Uncertainty	<0.01	*AOD*	0.01/ m
3. Pressure	<±5hPa	τ_{ray}	*0.0002 (862) – 0.0025(368)*
4. NO_2	±0.05nm	τ_{NO2}	*0(862) - 0.003(368)*
5. Ozone	± 10DU	τ_{O3}	0 (all) - 0.0003 (500)
6. Field of View	Depending on aerosol type and AOD	Meas. Voltage/AOD	0 – 0.12 (368, AOD=0.4, eff. Radius = 1.5μm)

The analysis of the table above includes:

- The uncertainty introduced in the measurement based on the standard deviation of the average of the 10 second measurement voltages for long term measurement analysis.
- The maximum calibration uncertainty including the triad stability, pointing differences within the calibration procedure and the calibration transfer.
- The uncertainty of the pressure reading of the PFR accompanied instrument.
- The NO_2 uncertainty taking into account the mean results of all GAW-PFR stations.
- The Ozone uncertainty based on OMI/Brewer differences and diurnal O_3 patterns.
- The Field of view related uncertainty. The results and numbers introduced for the uncertainty calculations have been derived from an analysis that is presented in the next section. The results here are shown for two $AODs_{500nm}$ [0.15 0.4] (global average and relatively high) and two aerosol mean effective radii [0.2 1.5] (μm) (small and large particles).

The total uncertainty as a function of the air mass is presented in figure 5.

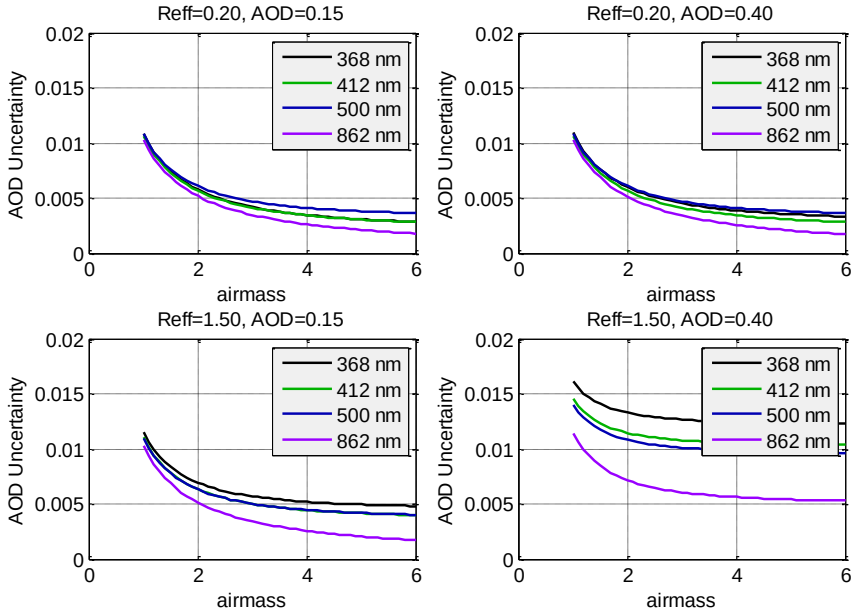

figure 5: Uncertainty estimation at the 4 PFR wavelengths as a function of air mass.

The four cases represented different AOD and mean effective radius (Reff) aerosol conditions.

Different cases are described in the header of each plot.

GCOS is currently reviewing and will update the requirements as part of their contribution to the UNFCCC Global Stocktake and the current state of the discussion is reflected on the web page "2022 requirement update". In this direction, results and experience gained from this GAW-PFR project were used for the definition of the new requirements that are under review. This project's PI S. Kazadzis is the main author of the GCOS requirements for AOD. The current, open for discussion, table of requirements is presented below.

The current open for discussion table of the GCOS – ECV requirements is presented below.

Table: AOD GCOS new requirements (open discussion)

Name	Multi-wavelength Aerosol Optical Depth		
Definition	Multi-wavelength AOD is the spectral dependent aerosol extinction coefficient integrated over the geometrical path length.(see note)		
Unit	Dimensionless		
Note	Aerosol Optical Depth quantifies the extinction of the radiation while propagating in an aerosol layer and reflects the aerosol loading information in the view of remote sensing measurement. AOD varies with wavelength and this variation is related to the aerosol size and type. The GAW guidelines recommend AOD be measured at 3 or more wavelengths among 368, 412, 500, 675, 778, and 862 nm with a bandwidth of 5nm. 1) under some assumptions of aerosol models and surface reflectance, spectral-dependence of AOD permits retrieval of Fine-AOD and Coarse-AOD, defined as the fraction of total aerosol optical depth attributed to the "non-dust" and "dust" aerosols, respectively, which are important parameters to distinguish aerosol type. 2) The absorption aerosol optical depth(AAOD) is the fraction of AOD related to light absorption and is defined as AAOD=(1−ωo)×AOD where ωo is the column integrated aerosol single scattering albedo.		
Requirements			
Item needed	**Unit**		**Value**
Horizontal Resolution	Km	Goal	50
		Breakthrough	100
		Threashold	500
Temporal Resolution	day	G	0.01
		B	1
		T	30
Timeliness	day	G	1
		B	7
		T	30
Required Measurement Uncertainty	% or AOD	G	2% or 0.01
		B	5% or 0.015
		T	10% or 0.03
Stability	%/decade or AOD/decade	G	1% or 0.005
		B	2% or 0.01
		T	5% or 0.02

Long term GAW-PFR data analysis

Based on the aims of the two phases we have initiated a study that had to deal with calibration, data correction and cloud flagging aspects discussed above. The study was based on the re-analysis of 11 years of one minute measurements of 3 reference PFRs at the high mountain station of Izana, Spain (IZO). The motivation of this work was based on the following facts:

- There has to be an independent comparison of different networks/instruments in order to assess the uncertainty analysis through the reasons for AOD differences.
- IZO is a GAW-PFR site and the instruments performing measurements are also reference instruments for GAW-PFR as they are periodically compared and re-evaluated the Davos reference triad (see phase 1)
- IZO is the European reference site that operates the AERONET (the densest aerosol network worldwide) standard instruments.
- Only short term comparisons and uncertainty analysis have been presented in the literature, so this 11 year more than 70.000 synchronous measurements dataset was unique in order to show the long term instrument performance.
- 15 different reference AERONET and 3 GAW-PFR instruments have been included in the analysis in order to assess the individual network stability.
- A large number of instruments worldwide is traceable to the compared instrumentation.

A comprehensive comparison of more than 70000 synchronous 1-minute aerosol optical depth (AOD) data from three Global Atmosphere Watch-Precision Filter Radiometers (GAW-PFR), traceable to the World AOD reference, and 15 Aerosol Robotic Network-Cimel (AERONET-Cimel, processing Versions V2 (old) and V3 (new)) radiometers, calibrated individually with the Langley plot technique, was performed for four common or near wavelengths 380 nm, 440 nm, 500 nm and 870 nm in the period 2005-2015.

Based on the decision of the Commission for Instruments and Methods of Observation (CIMO) of WMO (WMO, 2007) that recommended that the WORCC at the PMOD/WRC as the designated as the primary WMO Reference Centre for AOD measurements (WMO, 2005); the PFR instrument were treated as reference instrument in this study. For the comparison the WMO related uncertainties (percentage of data within the 0.005 + 0.01/m optical depths) have been used. The percentage of data meeting the WMO traceability requirements (95% of the AOD differences of an instrument compared to the WMO standards lie within specific limits) is > 92 % at 380 nm, > 95 % at 440 nm and 500 nm, and 98 % at 870 nm. (table and figure 6)

Channel	V2 (%)	V3 (%)
380 nm	92.7	92.3
440 nm	95.7	95.2
500 nm	95.8	95.7
870 nm	98.0	97.8

Percentage of AERONET-Cimel (V2 and V3) 1-minute AOD data meeting the WMO criteria for the four interpolated GAW-PFR channels for the period 2005-2015.

Percentage of AERONET-Cimel (V2 and V3) 1-minute AOD data meeting the WMO criteria for the four interpolated GAW-PFR channels for the period 2005-2015.

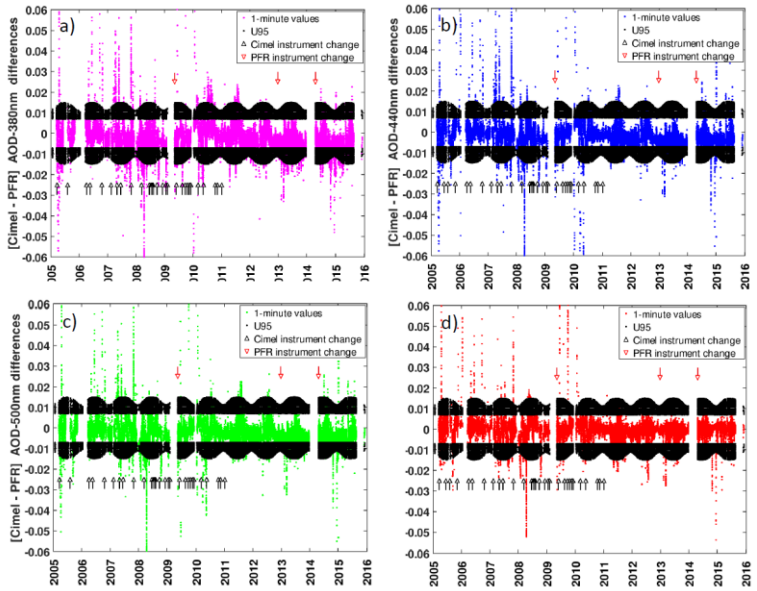

Figure 6. One-minute AOD data differences between AERONET-Cimel (V2) and GAW-PFR for (a) 380 nm (70838 data-pairs), (b) 440 nm (71645 data-pairs), (c) 500 nm (70833 data-pairs) and (d) 870 nm (71660 data-pairs) for the period 2005-2015. Black dots correspond to the U95 limits. A small number of outliers are out of the ±0.06 AOD differences range. Black arrows indicate a change of Reference AERONET-Cimel radiometer and red arrows indicate a change of the GAW-PFR instrument.

Traceability and uncertainty assessment

As presented in the previous table, data outside the WMO traceability criteria vary from 2% for 870 nm up to 7.3% for 380 nm. In this section, the different possible causes of non-traceability in AOD are evaluated and, if possible, quantitatively estimated.

Calibration related uncertainty

The calibration procedures of the AERONET-Cimel and GAW-PFR radiometers are different. As presented in the first section, in the case of GAW-PFR, frequent calibrations are established throughout the year and the calibration value is linearly interpolated in time, in AERONET- Cimel a constant calibration value is assumed in the intermediate period between two consecutive calibrations carried out on an annual basis. The typical calibration uncertainty for a single Langley plot is 0.7-0.9 % (at the 95 % confidence level), and it is reduced to 0.4 % in the case of IZO when averaging at least 10 Langley-derived extraterrestrial constants (which is the normal procedure) (Toledano et al., 2018). Regarding the GAW-PFR radiometers operated at IZO, a direct yearly comparison of the Langley based Vo's with the reference triad at PMOD/WRC showed differences lower than 1% for all channels for the 2005-2015 period.

In order to try to separate calibration related from other sources of uncertainties we used the fact (see formula 1) that calibration uncertainties affect AOD as a function of the air mass. For example, a not sufficiently accurate determination of the calibration constant results in a fictitious AOD diurnal evolution presenting a concave or convex characteristic curve symmetrical to local noon (minimum air mass). The largest error occurs in the central part of the day (lower air masses), mainly, in clean days with very low aerosol load (< 0.02 in 500 nm) as reported by Cachorro et al. (2004).

For the particular study, the total percentage of AOD traceable data pairs under pristine conditions (AOD500nm ≤ 0.03) was very high for all wavelengths (> 97.7 %) falling within the WMO limits, except for 380 nm. From the analysis of the remaining cases, under the conditions described above, it should be noted that ~ 44% of the cases with fictitious AOD diurnal cycles were due to small uncertainties in the calibration of AERONET-Cimel (V3), while for this same cause ~ 8% of cases were identified in GAW-PFR.

Cloud-screening uncertainties

Erroneous cloud screening is leading to the retrieval of artificially high AODs. We have examined the effect that the presence of clouds might have on AOD differences and the percentage of cases outside the WMO limits. The impact of clouds on AOD differences only occurs when cloud screening algorithms fail to identify clouds in the direct sun path. In order to assess the impact that cloud conditions might cause on AOD

traceability, we have used the concept of daily fractions of clear sky (FCS). FCS represents the percentage of observed sunshine hours in a day with respect to the maximum possible sunshine hours in that day. The higher the daily FCS, the higher the clear sky percentage we have on that day.

	380 nm	440 nm	500 nm	870 nm
0%≤FCS<20% (0.04%)	44.4	44.4	44.4	92.6
20%≤FCS<40% (0.22%)	76.6	82.2	80.8	94.1
40%≤FCS<60% (1.09%)	77.5	84.8	87.2	92.0
60%≤FCS<80% (7.17%)	89.6	93.9	94.4	97.6
FCS≥80% (91.5%)	92.8	95.6	96.1	98.1

Table: Percentage of AOD data within the U95 limits for each channel and 5 daily fractions of clear sky (FCS) intervals. In brackets, relative frequency of each FCS interval for AERONET V3.

It has to be noted that even if for high cloud percentages (FCS<60%) the percentage of data within the WMO limits is lower than for high FCSs, the percentage of data belonging in these groups is extremely low (<2%). Showing that improved (GAW-PFR and AERONET) cloud screening algorithms work very well.

Rayleigh scattering

The main errors in the calculation of Δτ Rayleigh from GAW-PFR can arise from errors in obtaining the atmospheric pressure. In this study, while AERONET-Cimel obtains the site station pressure from the National Centers for Environmental Prediction (NCEP) and the National Center for Atmospheric Research (NCAR) reanalysis at standard levels, GAW-PFR has a solid-state pressure transducer in the control box to read barometric pressure simultaneously with each PFR measurement. The results indicate that most of the 1-minute pressure differences are within ± 5 hPa, resulting in 1-minute ΔτR data within ± 0.001. So a negligible impact on the total AOD. However, there are a few cases that ΔτR increases significantly (∼ 0.01). It should be noted that out of >70K synchronous measurements only 99 data pairs have been registered for which the pressure difference between PFR and Cimel is greater than 20 hPa. These were cases of PFR barometric periodical malfunction or significant pressure changes during one day.

Differences in O3 absorption

The largest influence of total ozone data uncertainty in τO3 occurs at 500 nm. According to Wehrli (2008) and Kazadzis et al. (2018), total ozone needs to be determined to ± 30 DU or 10 % of typical values, to ensure an uncertainty of ± 0.001 in τO3 at 500 nm. In the case of the GAW-PFR / AERONET-Cimel comparison, and due to the very different method in which both networks obtained O3 values for their corresponding corrections, the ozone differences found on some days (1761 out of 71965 days; 2.4 %) are very large (> 40 DU), exceeding a difference in the ozone optical depth of 0.001. Even so, the potential contribution to AOD differences outside the WMO limits between the two networks is negligible. In the following figure the ozone related differences and their effects on AOD are presented:

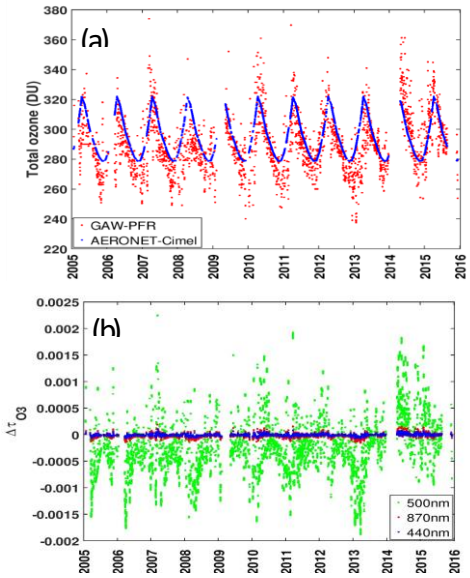

Figure 7. (a) Total O_3 used by GAW-PFR (measured Brewer O_3 values from IZO, OMI O_3 overpass or Brewer O_3 climatology) and AERONET-Cimel (TOMS O_3 climatology), and (b) $\Delta\tau_{O3}(\lambda)$ caused by differences in daily total O_3 between the two instruments in the period 2005-2015.

Differences in NO2 absorption

As mentioned in the previous section, NO2 contribution for GAW-PFR site can be considered neglibable. For this particular comparison, AERONET-Cimel applies a correction by absorption of NO2, but GAW-PFR does not include this correction. AERONET-Cimel V2 obtains daily total NO2 data from a 0.25° x 0.25° resolution NO2 monthly climatology obtained from the ESA Scanning Imaging Absorption SpectroMeter for Atmospheric CHartographY (SCIAMACHY) (Eskes and Boersma, 2003). In the following figure the effect of NO2 on AOD retrievals is shown. The effect becomes more important for lower wavelengths (380nm) and it is up to 0.002 for the highest NO2 period (May) at IZO.

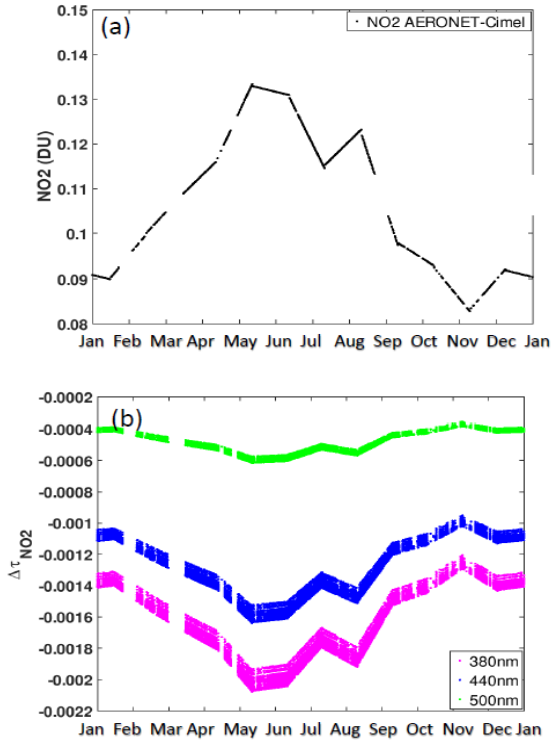

Figure 8. (a) NO_2 monthly climatology obtained from the ESA SCanning Imaging Absorption SpectroMeter for Atmospheric CHartographY (SCIAMACHY), used by AERONET-Cimel at IZO, and (b) $\Delta\tau_{NO2}(\lambda)$ caused by differences in daily total NO_2 between GAW-PFR and AERONET-Cimel in the period 2005-2015. Note that GAW-PFR does not take into account the correction for the NO_2 absorption

Instrument Field of view

An important issue that was discovered and analyzed in this study is the effect of the instrument field of view (FOV) in the AOD retrieval. PFR instruments have been developed according to the WMO guidelines having a fill angle FOV of 2.5 degrees. Having in mind that the apparent angle of the sun is ~0.5 degrees we have to consider that the forward scattering of aerosols from angles inside the PFR FOV and around the sun would lead to an increased (compared to the one that an instrument with 0.5 degrees FOV would measure) direct solar measurement. This introduces an uncertainty to the AOD determination that leads to systematically lower AOD retrievals. In order to assess this uncertainty, we have used: model calculations and comparison of the PFR instrument with a CIMEL (FOV= 1.3 degrees) instrument. Theoretically, this uncertainty increases under high AOD conditions and under aerosol types that favor forward scattering (e.g. dust particles). Taking advantage of the fact that Saharan dust intrusions regularly affect IZO, we provide a detailed analysis on the impact that dust forward scattering causes on the AOD retrieval of the two radiometers with different FOV, explaining the AOD differences under moderate-to-high dust load (AOD > 0.1) conditions. For this purpose, we have used a forward Monte Carlo model with which we perform simulations that include accurate dust aerosol near-forward scattering effects.

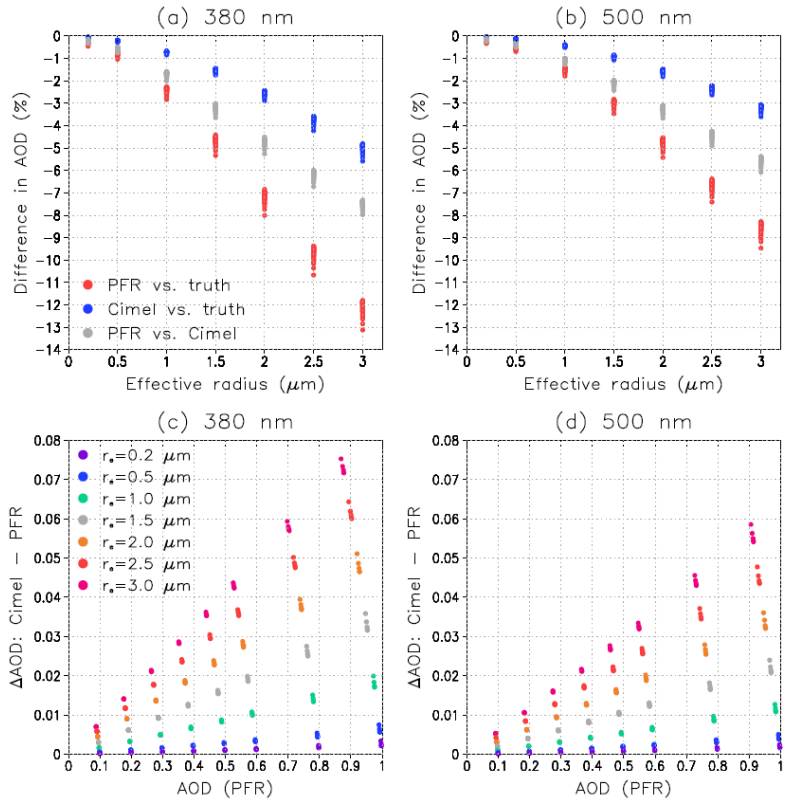

Figure 9. Panels a) and b): the simulated relative differences in retrieved AOD (in %) that would result from the scattered radiation within the FOV of the PFR and Cimel instruments. The red (blue) dots show the differences between the AOD that would be retrieved using PFR (Cimel) and the actual AOD, and the grey dots the difference between PFR and Cimel, at wavelengths (a) 380 nm and (b) 500 nm. Panels c) and d): the difference in retrieved AOD between PFR and Cimel, plotted as a function of the AOD retrieved with PFR, for seven values of aerosol effective radius between 0.2 and 3.0 μm, at (c) 380 nm and (d) 500 nm.

Based on these results the effect of FOV becomes important for AODs higher than 0.5 under conditions with very large aerosol particles. (e.g. mean dust particle radius for IZO is 1-1.5 μm).

Comparing PFR and CIMEL, the slopes of the fitting lines of the Cimel-PFR AOD differences vs. PFR AOD for AOD> 0.1 (dusty conditions), they are 2.7% for 380 nm and 2.3% for 500 nm, which are quite consistent with the model percentage differences of AOD between Cimel and PFR for an effective radius of 1.5 μm. These percentages correspond to absolute AOD differences of 0.016 at 380 nm, and 0.011 at 500 nm for AOD=0.5, that are of sufficient magnitude to cause an appreciable number of 1-minute AOD data outside the WMO limits.

If we apply the corresponding corrections to the 1-minute AOD PFR data > 0.1 assuming an effective radius of 1.5μm, + 3.3% at 380nm and + 2.2% at 500 nm, it turns out that the slopes of the fitting lines of the Cimel-PFR AOD differences vs. PFR AOD become practically zero. Moreover, the number of AOD data outside the WMO limits is reduced by approximately 53% for 380 nm and by 13% for 500 nm. It must be taken into account that the percentage of AOD data for AOD> 0.1 outside the U95 limits, before the corrections, is only 8% at 500 nm, while at 380 nm it is a significant value (24%).

Summary and Conclusions of the traceability study

While GAW-PFR is the WMO-defined global AOD reference, being directly linked to WMO / CIMO, and was specifically designed to detect long-term AOD trends, AERONET-Cimel is the densest AOD measurement network globally, and the network most frequently used for aerosol characterization and for model and satellite observation evaluation.

We have presented a long-term (2005-2015) 1-minute AOD comparison among different types of radiometers belonging to different aerosol global networks. This comparison is a very demanding test of both GAW-PFR and AERONET-Cimel validated AOD datasets since aerosol scenarios correspond to extreme conditions: either very low aerosol loading, a "pristine" scenario that reveals small uncertainties in the calibration and in the cloud screening, or large dust load, which leads to a significant increase in the forward scattering aerosol with AOD, resulting in a slightly higher AOD underestimation by the GAW-PFR. From this comprehensive comparison, we can conclude that both AOD datasets are representative of the same AOD population, which is a remarkable fact for the global aerosol community. It should be noted that AOD traceability at 380 nm (92.7 %) does not reach 95 % of the common data, the percentage recommended by WMO U95 criterion, so more efforts should be made to improve AOD in the UV range. In this study we have also investigated the data that are outside of the WMO U95 limits in order to understand their causes and to be eventually able to correct the small inconsistencies detected in instrumental and methodological aspects in the future. The results suggest that WMO/CIMO traceability limits could be redefined as a function of wavelength, and the recommended radiometer FOV range should be reconsidered. The widely deployed AERONET-Cimel and GAW-PFR datasets play a crucial role in understanding long-term AOD changes and detecting trends, so it would be desirable for both networks to be linked to the same GAW-WMO related reference.

GAW-PFR evolution

In addition, based on the results of this re-calibration and QA/QC study we reassessed the station locations in terms of AOD representativeness and to suggest possible instrument location changes for the future. This was based on:

- Technical problems, station close down.
- Geographical position
- Existing instruments in associated stations; calibrated the instruments with a frequency at least once per two years and to fulfil some basic quality control tests, related with the instrument maintenance at each site.
- Participating in Global or regional research infrastructure initiatives

Concerning the first category. Measurements at Bratts Lake. Canada have been stopped in 2013 and Ryori, Japan in 2019 due to the station close down (changed to automated station from the Jap. Meteor. Agency). Also, technical issues on the Danum Valley, Malaisia station (destruction of instrument, tracking system and data logging devices due to a thunderstorm) in 2017, resulted the end of the measurements. Finally, Mace Head, Ireland dataset have been stopped in 2016 due to a series of continuous instrument problems.

New stations included in the core GAW PFR stations were: Valentia, Ireland that comes to substitute the Mace Head, Ireland, with a dataset of more than 10 years. The Marambio (Finnish instrument) station in Antarctica, Troll station also in Antarctica and the initiation of updates in the Summit, Greenland station in order to be considered as a possible GAW-PFR station future inclusion.

A substitution of the Ryori station is planned to be a Chiba/Un. Of Chiba, Japan related station that cannot be considered as a continuation of the Ryori time series but a start of a new one linking the results with the ones of a main calibration site for the SKYNET network of instruments mainly active in Japan and Asia. Ryori station will continue measuring AODs using automatic instrumentation (SKYNET) that can be linked with Chiba measurements and provide a possibility of a homogeneous continuation of the series.

Two new instruments are going to be installed during early 2021 in two stations that are part of the ACTRIS (ACTRIS is the European Research Infrastructure for the observation of Aerosol, Clouds and Trace Gases) Calibration Center for Aerosol Remote Sensing (CARS) at Ohp/France and Valladolid/Spain. The installation of PFR instruments will be linked with the CARS/ACTRIS calibration activities and the long term measurements at the two sites. Other suggestions for new instrument locations will be discussed at the Scientific Advisory group of Aerosols of WMO which is the supervising scientific body for GAW-PFR.

New core stations:

Station (ab.)	Lat./Lon	Altitude (m)	Country	Type of Location	Main Types of Air-Masses	PFR Time-Series	Reason
Valentia (VAL)	51.94°N 10.24°W	24	Ireland	coast	marine boundary layer	2007 - present	Substitute of Mace Head Station
Marambio (MAR)	64.24°S 56.62°W	205	Argentina	coast	marine boundary layer	2005 - present	*South Hemisphere (Polar) station*
Troll (TRO)	72.01°S 2.54°E	1309	Antartica	polar	free-troposphere	2012-present	*South Hemisphere polar Station*

A major decision linked with the project results and contributing towards the future GAW-PFR evolution was the update of the whole network with a new series of PFR instruments, based on improved electronics and input optics technology. The new instruments are constructed in PMODWRC and will be ready in the end of 2020. Based on this plan all GAW-PFR station instruments will be replaced by the end of 2022 with the new instruments.

AOD climatology analysis

During this phase we have calculated statistics for each station including:

- The time series monthly and daily AODs at the 3 PFR wavelengths and Ångström exponent (AE). AE is calculated by fitting the 4 AODs
- The intra-annual variability of the AOD at 4 different wavelengths and the AE.
- The relative frequency distribution of the observed AODs together with the arithmetic mean and standard deviation and the geometrical mean and geometrical standard deviation of the distribution.
- The relative frequency distribution of AE together with the arithmetic mean and standard deviation
- The relationship of AOD at 500nm and the AE for daily averaged measurements.
- Related statistics (Average, standard deviation, median and 20-80 percentiles, geometrical mean and geometrical standard deviation, number of years, days). The numbers have been calculated using all available days.

The post processing methodology for retrieving AODs with the PFR instruments includes a number of tests that limit the number of measurements per day. Most important one in terms of data elimination is the cloud flagging which is performed in a minute basis as AOD cannot be measured with direct sun measurements through the clouds. In addition, sun pointing thresholds, AE variability thresholds, AOD wavelength based quality control are performed (see Kazadzis et al., 2018a)

A daily value of AOD is derived using at least 30 measurements that have passed all quality control and cloud flagging algorithms. Then a Monthly value is calculated using all measured points during the month with the restriction to have at least 10 available days (with some exceptions in mostly polar stations or months that the instrument was partly not working due to technical reasons). In all cases a manual inspection of the months not selected due to the 10-day criterion are investigated and decisions are made accordingly. For the

AOD measurements during a month, mean, median and geometrical mean values are calculated. The use of the average/media/geometrical mean has not been explored thoroughly in the literature. Most of the publications showing aerosol climatology use the average AODs on daily, monthly, annual scales. However, AOD is not normally distributed in such (e.g. monthly) time scales for most stations. Here we have calculated all three parameters (Mean, median, geometrical mean) and reported all results. The use of any of the averaging approach clearly depends on the actual application that someone would like to investigate. Such examples and more discussion on the aspect are presented in Sayer et al., 2019.

Statistics for each station have been generated over the whole measurement periods and have been included in Appendix I. An example of GAW-PFR measurements at Mauna Loa, USA and Jungfraujoch, Switzewrland stations are presented below:

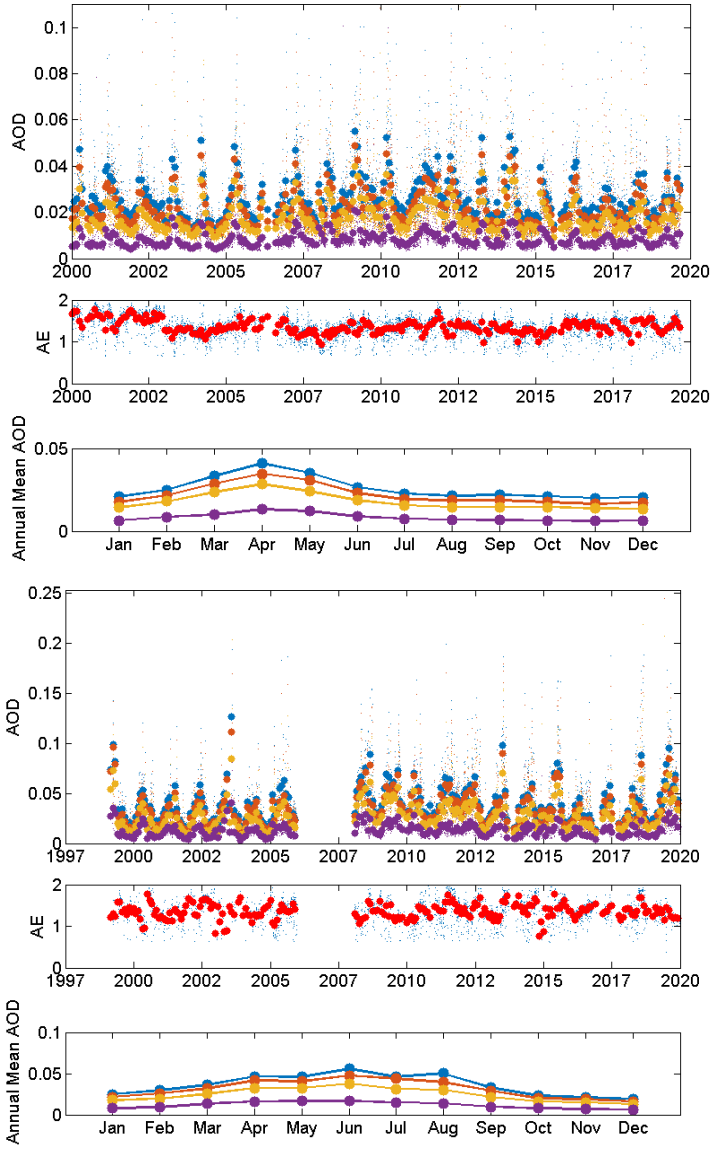

MAUNA LOA, USA

Period (Days) 2000 - 2019 (5827)

	Mean AOD ± std	Gm	med	Prc. 20 - 80
500nm	0.018 ± 0.013	0.016 /* 1.534	0.015	0.011 - 0.023
862nm	0.009 ± 0.006	0.007 /* 1.592	0.007	0.005 - 0.011
AE	1.348 ± 0.234	1.326 /* 1.206	1.357	1.165 - 1.544

JUNGFRAUJOCH, Switzerland

Period (Days) 1999 - 2019 (3020)

	Mean AOD ± std	Gm	med	Prc. 20 - 80
500nm	0.029 ± 0.020	0.025 /* 1.766	0.024	0.015 - 0.039
862nm	0.014 ± 0.010	0.012 /* 1.849	0.011	0.007 - 0.020
AE	1.350 ± 0.286	1.316 /* 1.263	1.375	1.110 - 1.598

Figure 10: Mauna Loa (up) and Jungfraujoch (down) time series of AOD at the 4 PFR wavelengths and AE and intra-annual AOD variability (left) and aerosol statistics (GM: geometrical mean, med: median, prc: percentiles) (right).

An overview of AOD and AE for the high altitude stations showed that mean and median AOD_{500nm} is decreasing with increasing altitude with the exception of Mountain Walliguan (WLG) station due to the dust related intrusions reported. AEs for Davos, Jungfraujoch and Mauna Loa are in the range of 1.3 to 1.4, very close to Ångström's classic value of 1.3 for natural aerosols. While for Izana (IZO) and WLG closer to 1.1 and

0.9 indicating an additional contribution of coarse aerosols with an AE smaller than 1. This can also be seen in a monthly level looking at the AOD – AE anti-correlation for July-August at IZO and February – May at WLG.

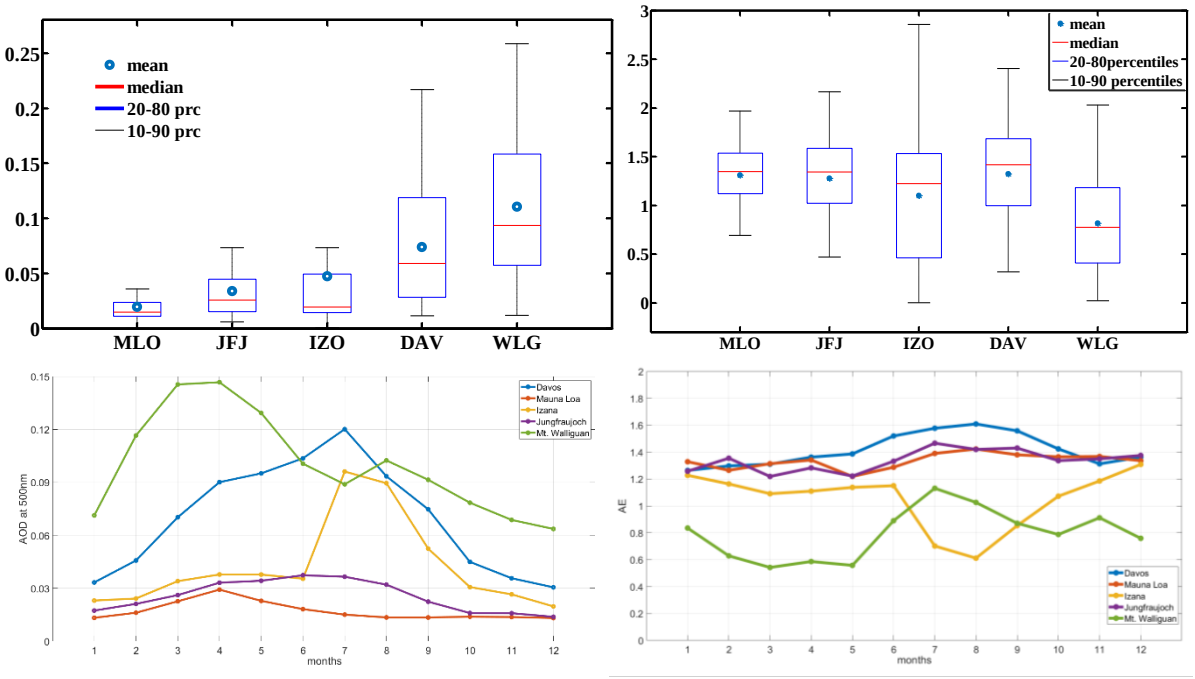

Figure 11: AOD_{500nm} (up-right) and AE (up-left) mean and median for 5 high altitude stations: (MLO-3.4Km, IZO-2.3Km, JFG 3.5Km, WLG-3.8Km, DAV-1.6Km). Intra-Annual monthly mean AOD at 500nm (down left) and AE (down right).

Trend analysis

Trend analysis was performed using two independent methods commonly used in the literature:

- The monthly/seasonal Kendall test, a generalization of the Mann-Kendall (MK) test, a non-parametric test that can be applied to time-series with seasonal cycles and missing values. The Seasonal Kendall test gives a statistic representing the "strength" and direction but not slope of the trend. The latter is determined by Sen's method which is robust to the influence of outliers as it takes the median value of all pairs of slope values. Hereafter mentioned as MK method) Data used were daily values of AODs, and AE from each GAW-PFR station.
- The Weatherhead et al., 1998 (WH) statistical method of trend detection that takes into account the magnitude of variability and autocorrelation of the noise in the data. Data used were monthly mean, median and geometrical mean of AODs at four wavelengths and AEs.

The MK method

An example of the MK test and Sen's slope for Mauna Loa station is provided below.

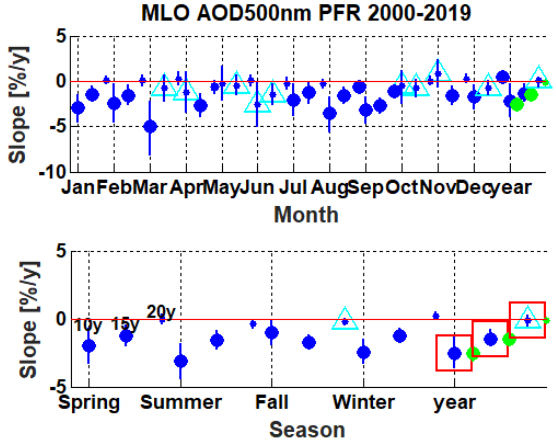

Figure 12. MK test and Sen's slope for AOD measurement at Mauna Loa, USA

Data shown in this plot can be interpreted as follows: Upper figure is the calculation of the monthly and total trends per year and lower the seasonal ones. Each month / season includes 3 points the 10 year the 15 year and the total (in this example is 20 years) trend. Statistically significant trends are plotted in big circles and non-significant in smaller circles. Red boxes show a homogeneous trend for the four meteorological seasons or for the 12 months. The green circles correspond to trend calculated directly from the whole time series, without considering seasons or months. Triangles show false positive or negative trends.

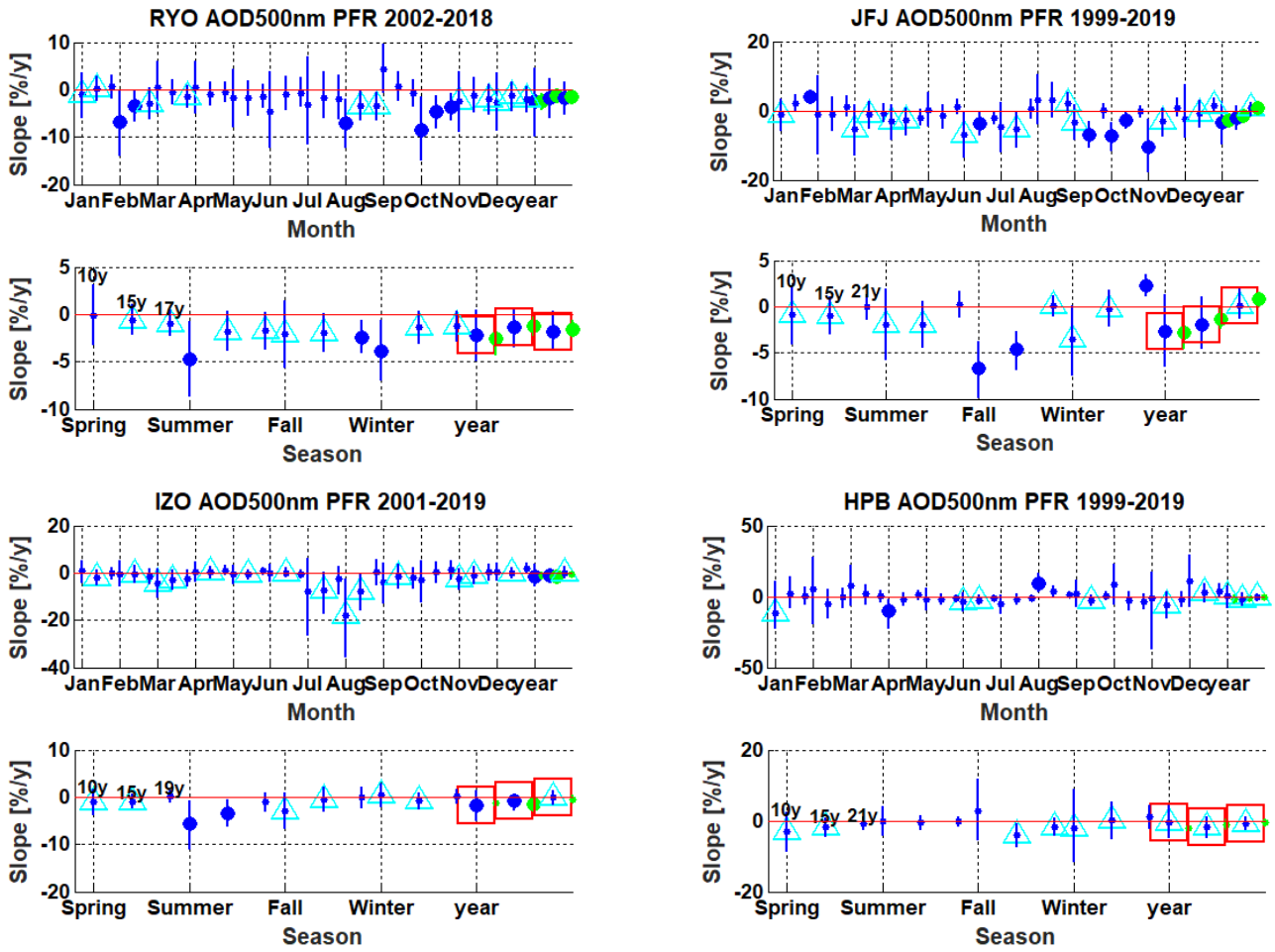

Figure 13: Results of the MK test for long term GAW-PFR time series: Ryori, Japan (up left), Jungfraujoch, Switzerland (up right), Izana, Spain (down left), Hohenpeissenberg, Germany (down right). Results are shown as trends for AOD per year for each month (up) and season (down) for different (10, 15, total year) periods. Larger circles represent 95% level statistical significant trends. Green points represent the trends without dividing the data to seasons. Red boxes represent trends that are homogeneous for the 4 meteorological seasons.

A table with all trend results using the MK test for the four PFR wavelengths and the AE is provided in Appendix I. A summary of the MK statistics results is provided below.

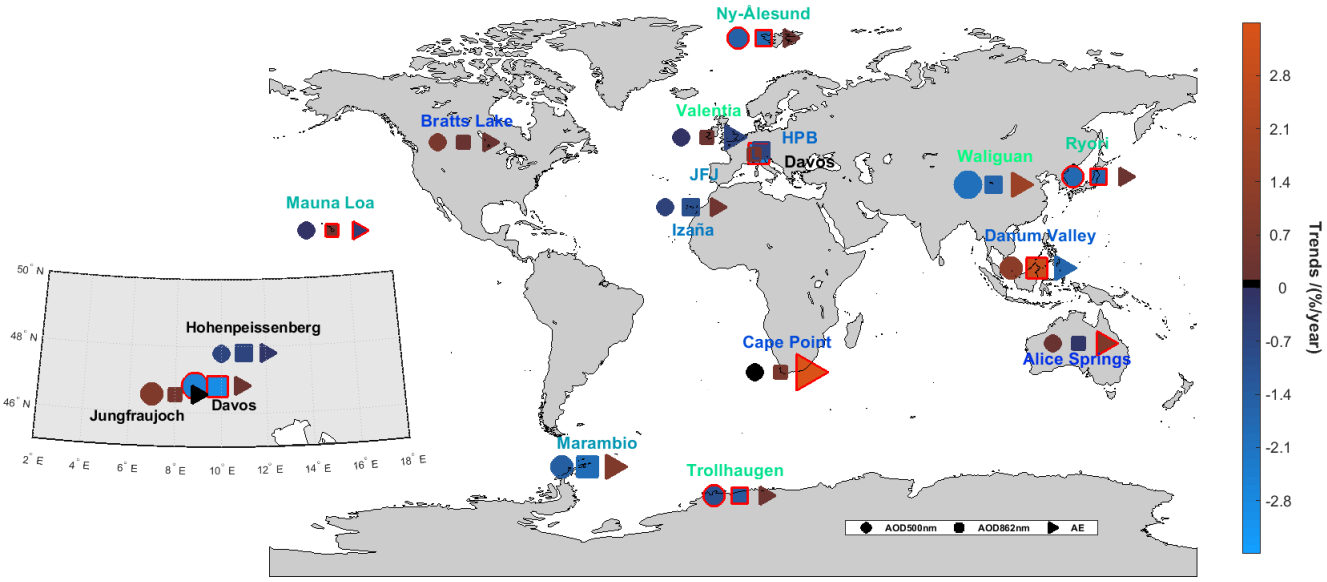

Figure 15: Map of trends per year for AOD at 500 (circle) and 865nm (box) and AE (triangle) using the MK test. Red outlined points show the 95% statistical significant values

The WH method

Conventional long-term trend detection of a time series is influenced by many factors such as the number of years of data, the magnitude of the uncertainty and autocorrelation of the noise (Weatherhead et al., 1998). The second approach to detect the GAW-PFR station trends was to use the WH method. We have calculated the trends per year (or per decade) and the percent trends using monthly (mean, geometrical mean and median) values of AODs in four wavelengths and the AE.

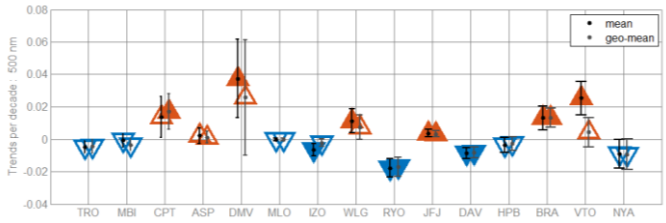

Figure 16a: trends per decade for AOD (mean and geometrical mean) at 500nm using the WH method

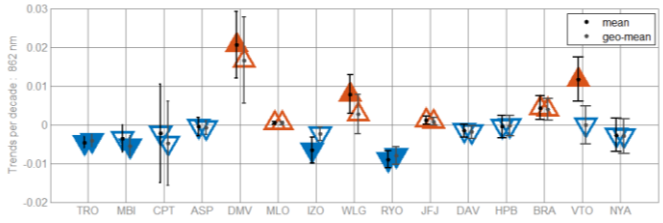

Figure 16b: trends per decade for AOD (mean and geometrical mean) at 862 nm using the WH method

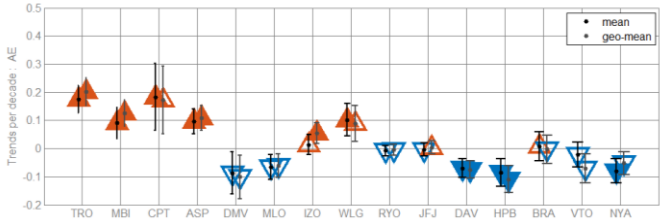

Figure 16c: trends per decade for AE (mean and geometrical mean) at 500nm using the WH method

Trends per decade among mean and geometrical mean values agree quite well. For most of the stations trends are low. The graphic shows mostly information to be interpreted for each individual station separately, as stations have different average AODs. Both absolute and percent trends and their statistical significance are presented in Appendix I comparing both MK and WH methods.

A figure showing the combination of the MK and the WH (3 quantities) results are shown below as fig. 17. The figure presents the % trends per year as calculated for AODs at 500nm and 865nm and for AE. In general, the two methods and four different approaches agree quite well. Defining the sign of the trend (positive or negative) the methods agree for 12 and 13 out of 15 stations for AOD_{550nm} and AE respectively.

The similar graph for absolute trends of AOD and AE is presented in Appendix I.

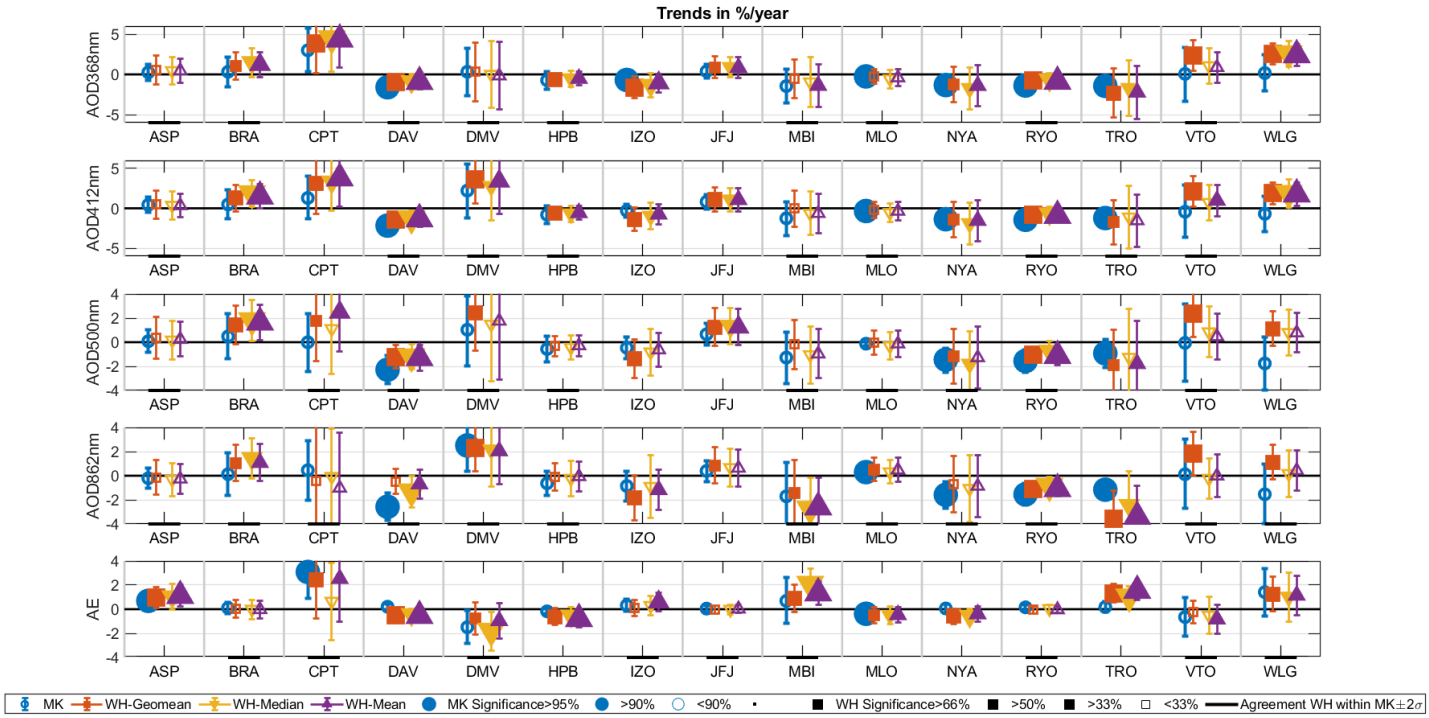

Figure 17: Trends in % per year for all stations. MK test (blue), WH test mean/median/geometrical mean (purple, yellow, red), full symbols stat. significant 90% (MK test), full squares stat. significant 50% (WH test).

Trends using satellite based retrievals

In addition to the GAW-PFR network data, satellite data have been used in this study.

The MODerate resolution Imaging Spectroradiometer (MODIS), mounted on the twin polar orbit satellites Terra and Aqua, operated by the National Aeronautics and Space Administration (NASA), acquires aerosol observations, among other geophysical parameters, since 2000 and 2002, respectively. The AODs have been produced by the latest available version of the MODIS retrieval algorithms (Collection 6.1, C061) and are provided at 10 km x 10 km nominal spatial resolution (Level 2, L2), QA=3 thus ensuring that only the most reliable data are utilized. For each PFR station, we are setting 10 concentric circles, centered at the station coordinates, with radii from 10 to 100 km increasing by a constant step of 10 km. Then, for each circle, we are calculating the regional mean and standard deviation, the coefficient of variation as well as the number of counts. At a further step, the regional means are used to compute the daily and monthly averages, the corresponding standard deviations as well as the number of counts, at each temporal scale. The aforementioned steps have been repeated for each station except Troll since MODIS does not provide AODs over snow-covered regions. MODIS data are accessible at the Level-1 and Atmosphere Archive & Distribution System (LAADS) Distributed Active Archive Center (DAAC) (https://ladsweb.modaps.eosdis.nasa.gov/).

Based on common days of existing measurements for PFR and MODIS Aqua/Terra data we have calculated the monthly and all data mean and geometrical means for each station. The main goal of this task was to try to investigate in trends per year using satellite based data agree with the ones presented with the GAW-PFR.

Comparing AOD data from both satellite based instruments with PFR data we have found differences that are related with the distance (radius) from the PFR station that MODIS data are averaged. Fig 18a shows the minimum absolute differences of MODIS Aqua and Terra minus PFR measurements at 550 and 500nm respectively. Minimum differences shown in triangles are within 0.03-0.04 for all stations with the exception

of the IZO and JFJ high mountain stations that the differences are larger than 0.08 which is a large number considering that the average long term AOD for these stations is less than half. Theoretically, this is anticipated as 20Km up to 100Km radius areas around the stations represent a much different aerosol atmosphere including lower altitudes and cities. In the case of Mauna Loa best agreement was found with the 10Km radius dataset (however this restricts a lot the number of points used). The difference is considerably getting larger with increasing area ending up to the levels of the other (IZO, JFJ) high altitude site levels. Circles in the figure represent MODIS-PFR normalized differences using the lower difference (triangle) as the normalization value. With the exception of MLO different areas contribute to the PFR-MODIS difference by less than 0.05. for most of the sites minimum differences are found in the 10 to 30 km radius areas results. Fig. 18b shows the geometrical means of all stations as calculated from PFR, and the two MODIS sensors.

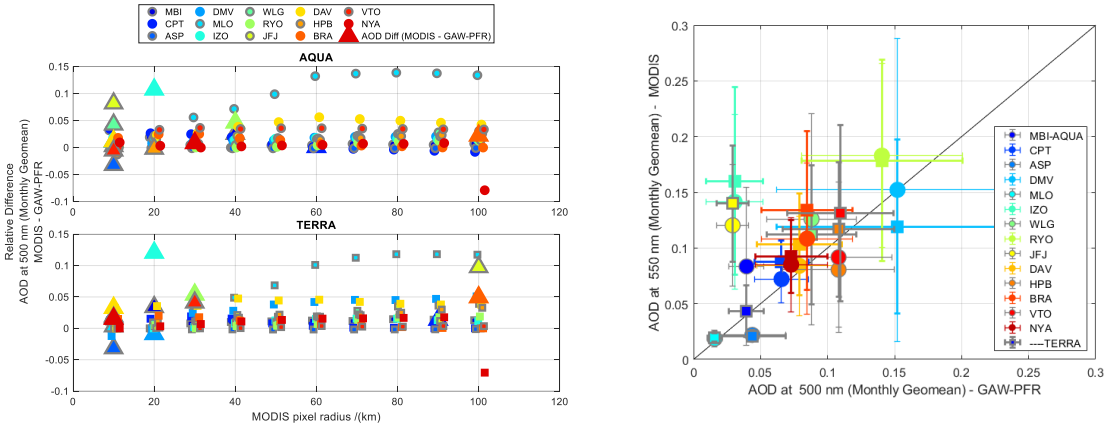

Figure 18. Left: MODIS-PFR difference for Aqua (up) and Terra (down) for different radius around the PFR stations for MODIS spatial integration. Triangles show the minimum AOD difference and circles the normalized (with the minimum) difference spatial integration related variability.

Using the common days of both MODIS and PFRs we have calculated monthly median AODs and trends using the WH method. Results show some reasonable agreement expressing the trend in AOD per decade.

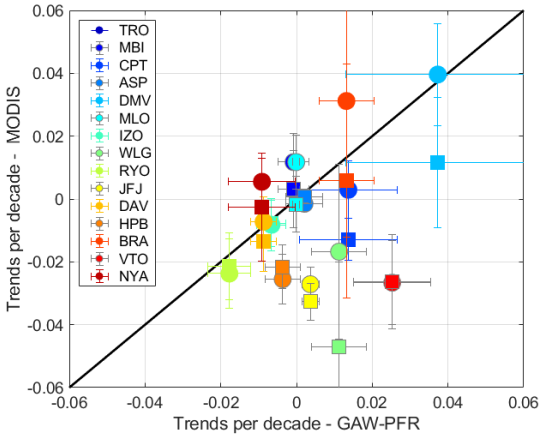

Figure 19: Trends of AOD per decade for MODIS (Terra-Boxes and Aqua-circles) and PFR measurements.

Conclusions of aerosol climatology and trend analysis

AOD at 4 wavelengths and AE retrieved using the sun-photometric measurements of PFR instruments belonging to the GAW-PFR network has been presented. In addition to arithmetic mean, geometric mean and median values have been calculated. Geometric means are much closer to the medians than arithmetic means. The AOD_{500nm} geometric standard deviation is of the order of 2, which means that AOD varies between 50% and 200% of the observed geometric mean, for all stations. At IZO, frequent Sahara dust events are responsible for a larger variability by a factor of 2.4-3 depending on the measured wavelength.

High mountain stations of MLO, JFJ and IZO showed the lowest AOD (0.018, 0.029, 0.049 for AOD500nm respectively) values, with the IZO measurements to show higher AODs and lower AEs at Saharan intrusion periods. WLG station exhibited high AODs and low AEs for a 4Km altitude stations. However, WLG is also affected by dust intrusions from middle China. AEs JFJ, MLO and DAV were found to be 1.3 to 1.4 that follow the Angstrom's suggestion for natural aerosols. ASP station had also low AOD_{500nm} values (0.056). The annual variation of AOD shows the standard pattern of low/high values in Austral winter/summer. Minimal daily means are comparable to high altitude stations in the northern hemisphere.

Most stations show larger AOD values in the summer than in winter months, with maximal values typically between spring and summer as rapid heating of the ground in spring and early summer leads to greater vertical instability, and consequently dust and combustion products are carried most effectively from ground to the atmosphere. The vegetation cycle or agricultural activities may further contribute to enhanced summer aerosol loads and introduce additional peaks during biomass burning periods (RYO, ASP, BRA).

Aerosol optical depth at polar stations Ny Ålesund is usually higher during spring than in summer. Spring time AODs at NYA are 2-3 times larger than the ones in the south polar stations of MBI and TRO. This is due to the Arctic haze phenomenon when aerosol removal mechanisms are suppressed and the cold and stable winter Arctic boundary layer may extend over anthropogenic sources in the south. Summer precipitation in NYA causes fast removal of accumulated aerosols and AOD values fall below continental values.

The monthly/seasonal Kendall test, a generalization of the Mann-Kendall (MK) test and the Sen's method for trend slope has been used for all PFR station daily data of four wavelengths and the AE. In addition, a second independent method. The Weatherhead et al., 1998 (WH) statistical method of trend detection that takes into account the magnitude of variability and autocorrelation of the noise in the data. Data used were monthly mean, median and geometrical mean of AODs at four wavelengths and AEs.

Using the MK test only 4 stations showed positive trends while none statistically significant ones. The remaining 11 stations showed generally small but negative trends all of them lower than 2% per year or 0.02 in AOD units per decade. High mountain stations showed small but negative trends (IZO, MLO, WLG) while JFJ showed a small but positive trend mostly associated with the second decade of measurements. In the cases of MLO, IZO and JFJ the AOD trend per decade is 0.001-0.002. 4 and 6 stations showed statistically significant trends for 500nm and 865nm wavelengths.

The WH results for mean, median and geometrical mean have been compared with the MK results. 13 out of 15 stations show an agreement on the trend sign for both methods (all three for WH and the MK). The two disagreeing stations did not have statistical significant trends for all methods. The agreement of the independent methods used gives more confidence on the result interpretation.

As reported applying new quality control and assurance procedures together with small improvements in the instrument calibrations led to these new time series of GAW-PFR stations. However, the lower limit of improving the data series is linked with the minimum uncertainties that the calibration and each of the methods used are introducing. Trend analysis results, especially the ones showing very low changes in AOD per decade have to be interpreted having in mind such uncertainty limitations. Further improvement of such QA/QC procedures in the future could introduce some small but non-significant change in the presented results.

Data submission in an open access database (WDCA)

GAW-PFR data are submitted regularly to WDCA. Real time data are sent in a daily basis. The current real time data utilize the new calibrations and QA/QC procedures that have been defined within this project. Data submission of recalibrated data to WDCA is performed according to WMO rules: full yearly dataset is submitted until the end of the following year unless a recalibration is pending (in this case immediately after the recalibration analysis).

Additional PFR stations mentioned here (Valentia/Ireland, Marambio and Troll/Antarctica) have been also started submitting data to the WDCA. One-minute data are not yet available in WDCA as at the moment hourly data are the maximum frequency data. New data series for all data from the GAW-PFR network are anticipated to be submitted and appear in the World Data Center for Aerosols till the end of 2020.

Outreach

- Presentation at the American Geophysical Union fall meeting, December, 2019 – San Fransisco, USA. Aerosol Optical Depth Measurements at the WMO Global Atmospheric Watch - PFR Network Stations

- Kazadzis, S., Kouremeti, N., and Groebner, J.: Aerosol Optical Depth Measurements at high altitude and polar WMO Global Atmospheric Watch - PFR Network Stations, EGU General Assembly 2020, Online, 4–8 May 2020, EGU2020-6161, https://doi.org/10.5194/egusphere-egu2020-6161, 2020

Online presentation: https://meetingorganizer.copernicus.org/EGU2020/EGU2020-6161.html

- The GAW-PFR network climatology and trends – PMODWRC Science meeting 07.2020, S. Kazadzis

Publication

- Cuevas, E., Romero-Campos, P. M., Kouremeti, N., Kazadzis, S., Räisänen, P., García, R. D., Barreto, A., Guirado-Fuentes, C., Ramos, R., Toledano, C., Almansa, F., and Gröbner, J.: Aerosol optical depth comparison between GAW-PFR and AERONET-Cimel radiometers from long-term (2005–2015) 1 min synchronous measurements, Atmos. Meas. Tech., 12, 4309–4337, https://doi.org/10.5194/amt-12-4309-2019, 2019.
- Nakajima, T., Campanelli, M., Che, H., Estellés, V., Irie, H., Kim, S.-W., Kim, J., Liu, D., Nishizawa, T., Pandithurai, G., Soni, V. K., Thana, B., Tugjsurn, N.-U., Aoki, K., Hashimoto, M., Higurashi, A., Kazadzis, S., Khatri, P., Kouremeti, N., Kudo, R., Marenco, F., Momoi, M., Ningombam, S. S., Ryder, C. L., and Uchiyama, A.: An overview and issues of the sky radiometer technology and SKYNET, Atmos. Meas. Tech. Discuss., https://doi.org/10.5194/amt-2020-72, 2020

Publication of data and results

A publication presenting the full climatology and trends of all GAW-PFR stations is going to be submitted in the fall of 2020. Data are regularly submitted to the World Data Center for Aerosols.

Acknowledgment: S. Kazadzis would like to thank Dr. Mar Martine Collaud Coen for the provision MK test and Sen's slope software and the help on the interpretation of the results.

References

Cuevas, E., Romero-Campos, P. M., Kouremeti, N., Kazadzis, S., García, R. D., Barreto, A., Guirado-Fuentes, C., Ramos, R., Toledano, C., Almansa, F., and Gröbner, J.: Aerosol Optical Depth comparison between GAW-PFR and AERONET-Cimel radiometers from long term (2005–2015) 1-minute synchronous measurements, Atmos. Meas. Tech. Discuss., https://doi.org/10.5194/amt-2018-438, accepted, 2019.

Kazadzis, S., Kouremeti, N., Diémoz, H., Gröbner, J., Forgan, B. W., Campanelli, M., Estellés, V., Lantz, K., Michalsky, J., Carlund, T., Cuevas, E., Toledano, C., Becker, R., Nyeki, S., Kosmopoulos, P. G., Tatsiankou, V., Vuilleumier, L., Denn, F. M., Ohkawara, N., Ijima, O., Goloub, P., Raptis, P. I., Milner, M., Behrens, K., Barreto, A., Martucci, G., Hall, E., Wendell, J., Fabbri, B. E., and Wehrli, C.: Results from the Fourth WMO Filter Radiometer Comparison for aerosol optical depth measurements, Atmospheric Chemistry and Physics, 18, 3185–3201, https://doi.org/10.5194/acp-18-3185-2018, 2018a.

Kazadzis, S., Kouremeti, N., Nyeki, S., Gröbner, J., and Wehrli, C.: The World Optical Depth Research and Calibration Center (WORCC) quality assurance and quality control of GAW-PFR AOD measurements, Geoscientific Instrumentation, Methods and Data Systems, 7, 39–53, https://doi.org/10.5194/gi-739-2018, https://www.geosci-instrum-method-data-syst.net/7/39/2018/, 2018b.

Mitchell, R. M., Forgan, B. W., and Campbell, S. K.: The Climatology of Australian Aerosol, Atmos. Chem. Phys., 17, 5131-5154, https://doi.org/10.5194/acp-17-5131-2017, 2017.

McPeters, R. D., Frith, S., and Labow, G. J.: OMI total column ozone: extending the long-term data record, Atmos. Meas. Tech., 8, 4845-4850, https://doi.org/10.5194/amt-8-4845-2015, 2015.

Toledano, C., González, R., Fuertes, D., Cuevas, E., Eck, T. F., Kazadzis, S., Kouremeti, N., Gröbner, J., Goloub, P., Blarel, L., Román, R., Barreto, A., Berjón, A., Holben, B. N., and Cachorro, V. E.: Assessment of Sun photometer Langley calibration at the high-elevation sites Mauna Loa and Izaña, Atmospheric Chemistry and Physics, 18, 14555–14567, https://doi.org/10.5194/acp-18-14555-2018, 2018.

Wehrli, C.: Calibrations of filter radiometers for determination of atmospheric optical depths, Metrologia, 37, 419-422, 2000.

WMO/GAW report No. 101, Report of the WMO workshop on the measurement of atmospheric optical depth and turbidity, (WMO TD No. 659), December 1993; Chapter: 4: Working Group Discussions – Sunphotometry (pp. 4-5), 1993

WMO/GAW report No. 227, WMO/GAW Aerosol Measurement Procedures, Guidelines and Recommendations, 2nd Edition, WMO- No. 1177, ISBN 978-92-63-11177-7, (WMO/TD- No. 1177), ISBN 978-92-63-11177-7, August 2016.; Chapter 7. Aerosol Optical Depth (pp. 60 - 67), 2016

WMO/GAW Report No. 231, The Fourth WMO Filter Radiometer Comparison (FRC-IV), November 2016

Che, H., Zhang, X.-Y., Xia, X., Goloub, P., Holben, B., Zhao, H., Wang, Y., Zhang, X.-C., Wang, H., Blarel, L., Damiri, B., Zhang, R., Deng, X., Ma, Y., Wang, T., Geng, F., Qi, B., Zhu, J., Yu, J., Chen, Q., and Shi, G.: Ground-based aerosol climatology of China: aerosol optical depths from the China Aerosol Remote Sensing Network (CARSNET) 2002–2013, Atmos. Chem. Phys., 15, 7619-7652, https://doi.org/10.5194/acp-15-7619-2015, 2015.

Goloub, P., Li, Z., Dubovik, O., Blarel, L., Podvin, T., Jankowiak, I., Lecoq, R., Deroo, C., Chatenet, B., Morel, J. P., Cuevas, E., and Ramos, R.: PHOTONS/AERONET sunphotometer network overview: description, activities, results, Proc. SPIE 6936, 69360V, doi:10.1117/12.783171, 2007.

Holben B.N., Tanré D., Smirnov A., Eck T.F., Slutsker I., Abuhassan N., Newcomb W.W., Schafer J.S., Chatenet B., Lavenu F., Kaufman Y.J., Vande Castle J., Setzer A., Markham B., Clark D., Frouin R., Halthore R., Karneli A., O'Neill N.T., Pietras C., Pinker R.T., Voss K., Zibordi G.: An emerging ground-based aerosol climatology: Aerosol optical depth from AERONET, J. Geophys. Res., 106, 12067–12097, 2001.

Mitchell, R. M., Forgan, B. W., and Campbell, S. K.: The Climatology of Australian Aerosol, Atmos. Chem. Phys., 17, 5131-5154, https://doi.org/10.5194/acp-17-5131-2017, 2017.

Wehrli, C.: Calibrations of filter radiometers for determination of atmospheric optical depths, Metrologia, 37, 419-422, 2000.

IPCC: Working Group I Contribution to the IPCC Fifth Assessment Report Climate Change 2013: The Physical Science Basis, Summary for Policymakers, IPCC, Geneva, Switzerland, Final Draft pp., 2013.

Nakajima, T., Campanelli, M., Che, H., Estellés, V., Irie, H., Kim, S.-W., Kim, J., Liu, D., Nishizawa, T., Pandithurai, G., Soni, V. K., Thana, B., Tugjsurn, N.-U., Aoki, K., Hashimoto, M., Higurashi, A., Kazadzis, S., Khatri, P., Kouremeti, N., Kudo, R., Marenco, F., Momoi, M., Ningombam, S. S., Ryder, C. L., and Uchiyama, A.: An overview and issues of the sky radiometer technology and SKYNET, Atmos. Meas. Tech. Discuss., https://doi.org/10.5194/amt-2020-72, 2020.

APPENDIX I

Overview of all climatology related statistics of all stations of the GAW-PFR network.

	Mean AOD ± std	Gm	med	perc20 - perc80		Mean AOD ± std	Gm	med	perc20 - perc80
ASP	**Period (Days)**			2002 - 2019 (4861)	**MBI**	**Period (Days)**			2005 - 2016 (491)
500nm	0.056 ± 0.049	0.044 /* 1.933	0.041	0.025 - 0.076	500nm	0.040 ± 0.039	0.034 /* 1.625	0.032	0.023 - 0.047
862nm	0.033 ± 0.026	0.026 /* 1.910	0.025	0.015 - 0.046	862nm	0.025 ± 0.035	0.019 /* 1.891	0.018	0.011 - 0.030
AE	1.006 ± 0.326	0.948 /* 1.434	1.003	0.707 - 1.304	AE	1.010 ± 0.347	0.950 /* 1.430	0.980	0.675 - 1.316
BRA				2001 - 2011 (2468)	**MLO**				2000 - 2019 (5827)
500nm	0.097 ± 0.072	0.079 /* 1.896	0.077	0.047 - 0.134	500nm	0.018 ± 0.013	0.016 /* 1.534	0.015	0.011 - 0.023
862nm	0.043 ± 0.030	0.036 /* 1.870	0.035	0.021 - 0.061	862nm	0.009 ± 0.006	0.007 /* 1.592	0.007	0.005 - 0.011
AE	1.410 ± 0.266	1.383 /* 1.222	1.430	1.162 - 1.652	AE	1.348 ± 0.234	1.326 /* 1.206	1.357	1.165 - 1.544
CPT				2010 - 2018 (1492)	**NYA**				2002 - 2019 (1568)
500nm	0.077 ± 0.052	0.065 /* 1.707	0.062	0.042 - 0.098	500nm	0.079 ± 0.046	0.069 /* 1.671	0.067	0.044 - 0.108
862nm	0.053 ± 0.031	0.045 /* 1.741	0.045	0.029 - 0.073	862nm	0.038 ± 0.027	0.031 /* 1.780	0.031	0.018 - 0.052
AE	0.746 ± 0.366	0.654 /* 1.704	0.698	0.401 - 1.053	AE	1.346 ± 0.301	1.304 /* 1.313	1.406	1.111 - 1.609
DAV				2003 - 2019 (3505)	**RYO**				2002 - 2018 (3499)
500nm	0.075 ± 0.056	0.058 /* 2.079	0.057	0.029 - 0.118	500nm	0.163 ± 0.107	0.133 /* 1.897	0.129	0.074 - 0.246
862nm	0.034 ± 0.026	0.025 /* 2.150	0.025	0.012 - 0.051	862nm	0.078 ± 0.051	0.064 /* 1.910	0.062	0.035 - 0.120
AE	1.421 ± 0.320	1.378 /* 1.303	1.471	1.171 - 1.707	AE	1.347 ± 0.247	1.322 /* 1.218	1.371	1.139 - 1.560
DMV				2007 - 2015 (907)	**TRO**				2007 - 2019 (1757)
500nm	0.156 ± 0.079	0.139 /* 1.630	0.141	0.089 - 0.212	500nm	0.025 ± 0.011	0.023 /* 1.439	0.022	0.017 - 0.030
862nm	0.088 ± 0.046	0.076 /* 1.743	0.081	0.046 - 0.129	862nm	0.012 ± 0.008	0.011 /* 1.567	0.010	0.008 - 0.015
AE	1.164 ± 0.427	1.070 /* 1.553	1.219	0.741 - 1.578	AE	1.351 ± 0.288	1.315 /* 1.276	1.400	1.108 - 1.595
HPB				1999 - 2019 (3339)	**VTO**				2007 - 2017 (964)
500nm	0.120 ± 0.089	0.092 /* 2.161	0.099	0.044 - 0.185	500nm	0.116 ± 0.073	0.098 /* 1.781	0.098	0.059 - 0.157
862nm	0.054 ± 0.045	0.040 /* 2.248	0.042	0.019 - 0.081	862nm	0.068 ± 0.040	0.057 /* 1.792	0.058	0.035 - 0.094
AE	1.429 ± 0.355	1.364 /* 1.415	1.509	1.166 - 1.731	AE	0.951 ± 0.327	0.896 /* 1.412	0.880	0.624 - 1.285
IZO				2001 - 2019 (5698)	**WLG**				2008 - 2017 (1273)

500nm	0.049 ± 0.068	0.030 /* 2.433	0.024	0.015 - 0.059	500nm	0.101 ± 0.056	0.087 /* 1.731	0.088	0.054 - 0.140
862nm	0.037 ± 0.063	0.017 /* 3.095	0.012	0.007 - 0.043	862nm	0.069 ± 0.043	0.057 /* 1.889	0.058	0.032 - 0.101
AE	1.048 ± 0.503	0.862 /* 2.071	1.167	0.472 - 1.495	AE	0.828 ± 0.346	0.760 /* 1.520	0.780	0.487 - 1.104
JFJ				1999 - 2019 (3020)					
500nm	0.029 ± 0.020	0.025 /* 1.766	0.024	0.015 - 0.039					
862nm	0.014 ± 0.010	0.012 /* 1.849	0.011	0.007 - 0.020					
AE	1.350 ± 0.286	1.316 /* 1.263	1.375	1.110 - 1.598					

Tables with AOD and AE trend results. MK: Mann- Kendal, WH: Weatherhead et al., 1998. Blue statistically significant 66% (WH) and blue statistically significant 95%*

AOD 500nm		**Trends**	**(%/year)**	**Trend (x1E-2 AOD/year)**
Station	**Years**	**MK ± 2 sigma**	**WH ± 2 sigma**	**MK**
ASP	18	0.086 ± 0.942	0.247 ± 0.719	0.002
BRA	11	0.477 ± 1.857	**1.649 ± 0.742***	0.021
CPT	9	-0.005 ± 2.414	2.479 ± 1.612	0.000
DAV	17	**-2.278 ± 1.159***	**-1.300 ± 0.518***	**-0.067***
DMV	9	1.035 ± 2.914	1.760 ± 2.420	0.090
HPB	21	-0.561 ± 1.055	-0.286 ± 0.437	-0.033
IZO	19	-0.465 ± 0.895	-0.624 ± 0.698	-0.006
JFJ	21	0.659 ± 0.894	1.250 ± 0.756	0.008
MBI	12	-1.276 ± 2.138	-0.965 ± 1.017	-0.033
MLO	20	-0.124 ± 0.186	-0.134 ± 0.540	-0.001
NYA	18	**-1.447 ± 0.997***	-1.273 ± 1.286	**-0.061***
RYO	17	**-1.559 ± 0.909***	**-1.124 ± 0.383***	**-0.139***
TRO	13	**-0.922 ± 1.186***	-1.781 ± 1.772	**-0.012***
VTO	11	-0.055 ± 3.180	0.462 ± 0.960	-0.003
WLG	10	-1.760 ± 2.209	0.785 ± 0.818	-0.086

AOD 865nm		**Trends**	**(%/year)**	**Trend (x1E-2 AOD/year)**
Station	**Years**	**MK ± 2 sigma**	**WH ± 2 sigma**	**MK**
ASP	18	-0.207 ± 0.814	-0.269 ± 0.612	-0.003
BRA	11	0.129 ± 1.759	1.082 ± 0.774	0.003
CPT	9	0.458 ± 2.497	-1.020 ± 2.304	0.013
DAV	17	**-2.576 ± 1.138***	-0.693 ± 0.601	**-0.035***
DMV	9	**2.507 ± 2.145***	2.053 ± 1.379	**0.148***
HPB	21	-0.628 ± 0.992	-0.068 ± 0.627	-0.016
IZO	19	-0.852 ± 1.228	-1.167 ± 0.848	-0.005
JFJ	21	0.396 ± 0.873	0.636 ± 0.774	0.002
MBI	12	-1.708 ± 2.929	**-2.606 ± 1.234***	-0.023

MLO	20	**0.296 ± 0.213***	0.481 ± 0.501	**0.002***
NYA	18	**-1.585 ± 1.095***	-0.860 ± 1.285	**-0.028***
RYO	17	**-1.545 ± 0.901***	**-1.093 ± 0.313***	**-0.066***
TRO	13	**-1.159 ± 0.760***	**-3.386 ± 1.293***	**-0.008***
VTO	11	0.120 ± 2.849	-0.013 ± 0.893	0.004
WLG	10	-1.538 ± 2.457	0.435 ± 0.822	-0.051

AE		**Trends**	**(%/year)**	**Trend (x0.1 AE/yr)**
Station	**Years**	**MK ± 2 sigma**	**WH ± 2 sigma**	**MK**
ASP	18	**0.693 ± 0.383***	**1.117 ± 0.452***	**0.044***
BRA	11	0.109 ± 0.486	-0.025 ± 0.366	0.011
CPT	9	**3.089 ± 2.168***	2.534 ± 1.786	**0.167**
DAV	17	0.205 ± 0.249	**-0.545 ± 0.218***	0.021
DMV	9	-1.488 ± 1.363	-0.953 ± 0.731	-0.143
HPB	21	-0.175 ± 0.220	**-0.803 ± 0.349***	-0.018
IZO	19	0.323 ± 0.476	0.590 ± 0.392	0.024
JFJ	21	0.049 ± 0.244	0.025 ± 0.179	0.005
MBI	12	0.689 ± 1.909	**1.333 ± 0.491***	0.047
MLO	20	**-0.380 ± 0.134***	-0.462 ± 0.316	**-0.034**
NYA	18	0.065 ± 0.349	-0.400 ± 0.308	0.006
RYO	17	0.156 ± 0.231	-0.036 ± 0.144	0.015
TRO	13	0.176 ± 0.422	**1.543 ± 0.372***	0.017
VTO	11	-0.649 ± 1.621	-0.819 ± 0.592	-0.046
WLG	10	1.415 ± 1.941	1.153 ± 0.822	0.076

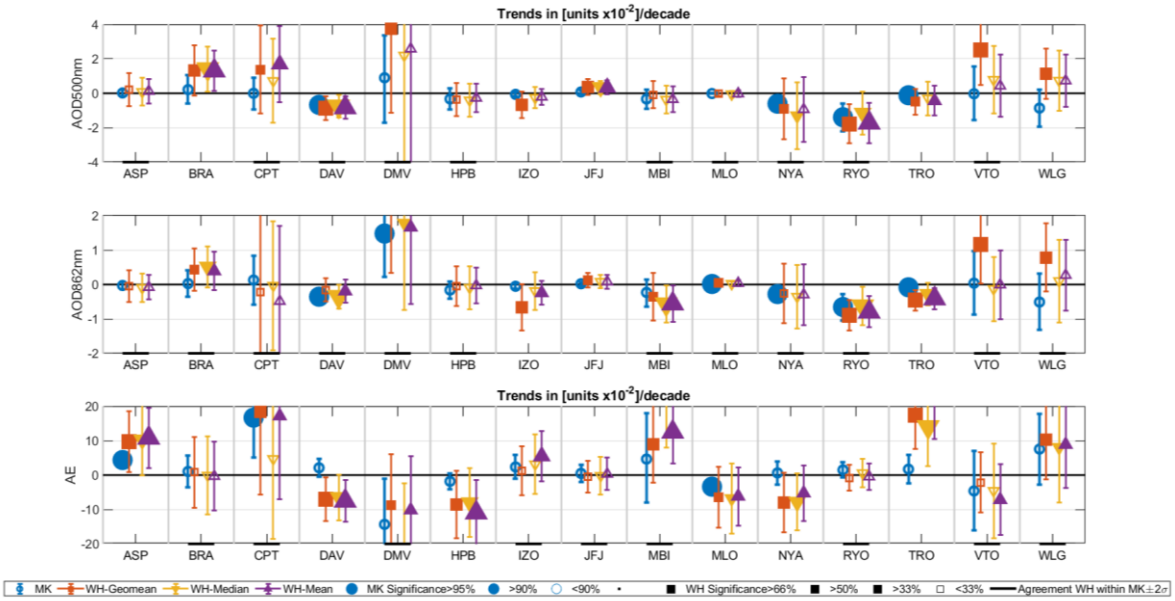

Trends in AOD and AE units per year for all stations. MK test (blue), WH test mean/median/geometrical mean (purple, yellow, red), full symbols stat. significant 90% (MK test), full squares stat. significant 50% (WH test).